NASA TECHNICAL TRANSLATION NASA TT F-13,463

APPLICATION OF A MIXING LENGTH SCHEME TO THE STUDY OF EQUILIBRIUM TURBULENT BOUNDARY LAYERS

Roger Michel, Claude Quemard, and Roland Durant

Translation of "Application d'un schema de longueur de melange a l'etude des couches limites turbulentes d'equilibre". Office National D'Etudes et de Recherches Aerospatiales, Paris, France, Technical Note No. 154, 1969, 57 pages.

NATIONAL AERONAUTICS AND SPACE ADMINISTRATION
WASHINGTON, D. C. 20546 FEBRUARY 1971

0 - PRINCIPAL SYMBOLS USED

x	:	logitudinal coordinate
y	:	normal coordinate at the wall
η	:	$\frac{y}{\delta}$; $y^+ = \frac{\rho_p u_\tau y}{\mu_p}$
l	:	mixing length; $L = l/\delta$
k	:	coefficient of $l = ky$ $(k = 0{,}41)$
u	:	longitudinal component of velocity
u_τ	:	friction speed $(\tau_p/\rho_p)^{1/2}$
u^+	:	$= \frac{u}{u_\tau}$
V	:	transformed velocity $V^+ = \frac{V}{u_\tau}$
f'	:	deficient velocity $\frac{V_e - V}{u_\tau}$
v	:	normal component of velocity
v_p	:	parietal injection speed $v_p^+ = \frac{v_p}{u_\tau}$
M	:	Mach number
p	:	pressure
ρ	:	density
T	:	temperature
h	:	enthalpy
h_i	:	stagnation enthalpy $h + \frac{u^2}{2}$
h_{it}	:	turbulent stagnation enthalpy $h + \mathcal{P}_t \frac{u^2}{2}$
H	:	transformed enthalpy $H^+ = \frac{H}{\mathcal{P}_t H_\tau}$
H_τ	:	friction enthalpy $\frac{\phi_p u_\tau}{t_p}$
μ	:	viscosity $\nu = \frac{\mu}{\rho}$
λ	:	heat conductivity
ε	:	turbulent viscosity

χ	:	turbulent conductivity
$\mathcal{P}$	:	Pradtl number $\mu c_p / \lambda$
$\mathcal{P}_t$	:	turbulent Pradtl number $\varepsilon c_p / \chi$
δ	:	thickness of boundary layer
δ^*	:	displacement thickness
Θ	:	momentum thickness
$\bar{\delta}^*, \bar{\theta}$	:	transformed thickness
$\mathcal{R}_\delta, \mathcal{R}_{\delta^*}$	:	Reynolds numbers
$\overline{\mathcal{R}_\delta}, \overline{\mathcal{R}_{\delta^*}}$	:	transformed Reynolds numbers
τ	:	friction in the boundary layer $= \tau_t + \tau_l$
τ_l	:	laminar friction : $\mu \frac{\partial u}{\partial y}$
τ_t	:	turbulent friction : $-\overline{(\rho v)' u'}$
ϕ	:	heat flux in the boundary layer $= \phi_l + \phi_t$
ϕ_l	:	laminary heat flux $-\lambda \frac{\partial T}{\partial y}$
ϕ_t	:	turbulent heat flux $\overline{(\rho v)' h'}$
τ_p	:	friction at the wall
ϕ_p	:	heat flux at the wall
C_f	:	friction coefficient $2\tau_p / \rho_e u_e^2$
$\overline{C_f}$	:	transformed friction coefficient
$\overline{C_h}$	:	transformed heat flux coefficient
$\overline{\mathcal{S}}$	:	$\frac{2\overline{C_h}}{\overline{C_f}}$ analogy factor
β	:	pressure gradient parameter
$\bar{\beta}$	:	transformed parameter
$\mathcal{P}$	:	injection parameter $\rho v_p u_e / \tau_p$

Subscripts

e	:	conditions at the edge of the boundary layer
p	:	conditions at the wall
ℓ	:	laminar measurements
t	:	turbulent measurements

APPLICATION OF A MIXING LENGTH SCHEME TO THE STUDY OF EQUILIBRIUM TURBULENT BOUNDARY LAYERS

Roger Michel, Claude Quemard, and Roland Durant

ABSTRACT. A turbulence scheme, based on an improved concept of mixing length, is applied to equilibrium turbulent boundary layers.

Assuming an incompressible flow, the velocity profiles of a boundary layer subjected to both pressure gradient and fluid transfer at the wall are determined, as well as the influence of these two parameters on the wall friction.

This treatment is extended to the compressible case. The laws are established for the velocity and enthalpy profiles. It is shown that pressure gradients have a considerable influence on the value of the Reynolds analogy factor.

I. INTRODUCTION

The variety of boundary conditions concerned and the complexity of the /5* results relative to turbulent boundary layers in recent supersonic and hypersonic problems have shown that it is becoming increasingly delicate and problematical to resort to the approximate techniques utilized so far, which involve the empirical extension of incompressible results.

It is thus deemed necessary to avail ourselves of more thorough analytical methods and take into consideration as much as possible the properties linked to turbulence structure. For this purpose, a scheme was drawn up based on the classical concept of mixing length and involving essentially an improvement over customary hypotheses.

---

*Numbers in the margin indicate pagination in the original foreign text.

It first proved true that a really convincing check on the hypotheses in this scheme could only come with a comparison of the results to which it leads, with a sufficient number of coherent experiments, and that this check should be first carried out in an incompressible fluid. The special opportunity presented itself at the conference on calculating turbulent boundary layers held at Stanford University in 1968, where we were allowed to present and compare with experimental data a method of calculation based on the application of the scheme to incompressible equilibrium boundary layers [1].

It later appeared possible to extend the treatment to the case of a fluid transfer at the wall. Attention was turned to the case of a compressible fluid where it was possible to make a parallel application to thermal boundary layers.

Thus, we have a set of results by which we can analyze in a systematic manner the effects of the principal factors which may act on the development of a turbulent boundary layer and on the friction and heat transfer caused by it.

II. HYPOTHESES AND RESEARCH PRINCIPLES

II.1. Proposed scheme for mixing length

II.1.1. Modifications Required in Customary Hypotheses

In order to obtain an expression for turbulent friction as a basis which will allow us to study the problems involving the conditions at the various boundaries, the scheme to be proposed is based on the classical concept of mixing length. We have sought only to modify certain hypotheses so as to take /6 into account the properties brought to light which are quite obvious from experimental data.

The criticisms which should be made of the customary hypotheses will first be summarized in three points:

— The classical application of the concept is from the outset limited to the part of the flow for which friction is made up essentially of the turbulent term.

— Since the concept of mixing length is originally applied to longitudinal fluctuation u' of velocity, it should always be more or less explicitly supposed that vertical fluctuation v' is proportional to it or that the turbulent friction is proportional to turbulence intensity, to end up with the usual expression

$$\tau_t = -(\rho v)' u' = \rho l^2 \left(\frac{\partial u}{\partial y}\right)^2; \qquad \text{(II.1)}$$

Experience shows that this proportionality exists in the greater part of the boundary layer; it also shows, however, that it no longer holds in the vicinity of the wall and that the ratio of turbulent friction to turbulence intensity tends towards zero with distance to the wall.

— Except in recent treatments, the hypothesis regarding the evolution of mixing length has hardly been worked out, or at any rate, has hardly been used except in the vicinity of the wall. If it is generally accepted that mixing length is proportional to y at slight distances from the wall, it is also sufficiently clear that it should subsequently vary in a manner which differs from it considerably.

In view of these criticisms, we propose to make the following modifications in the hypotheses:

Friction will involve generally not only the turbulence term, but also the viscosity term; the turbulence term should be expressed so that it reflects the fact that its ratio to the turbulence intensity tends toward zero at the wall. Thus, the following formula is used for total friction:

$$\tau = \mu \frac{\partial u}{\partial y} + F^2 \rho l^2 \left(\frac{\partial u}{\partial y}\right)^2 \qquad \text{(II.2)}$$

where F^2 is a corrective function which should be zero at the wall; it intervenes essentially in the viscous sub-layer and becomes one, so that the expression for turbulent friction regains the classical form of the mixing length concept when the turbulence term has become more important than the viscosity term.

It is still granted that mixing length is of the form $l = ky$ near the wall, with a universal coefficient k on the order of 0.4; however, the mixing length will diverge from this relationship as the distance increases; the slipstream serves as an example suggesting that we look for an evolution which makes l tend toward a constant value characteristic of the dimension of eddies in the outer part of the boundary layer.

The work dealt with the two essential points:

— determination of a reasonable hypothesis for the variation in mixing length in the entire boundary layer; /7

— determination of the correcting function F^2 which represents the effects of proximity of the wall on the ratio of v' to u', and consequently, on the expression for turbulent friction.

In fact, there were no other methods than empirical ones for finding these two elements, and they were initially obtained through experimental data. It should be noted, however, that we sought to reduce to a minimum this report to empiricism; only as a result of findings on a flat sheet (or cylindrical drive) turbulent boundary layer in an incompressible fluid were the hypotheses established on mixing length and the viscous sub-layer correcting function. Applications to such other cases as pressure gradient, fluid transfer at the wall, fluid compressibility later confirmed that the hypotheses were actually of sufficiently wide scope.

II.1.2. Universal mixing length curve

The fundamental hypothesis is that mixing length is a universal function of distance to the wall, when l and y are related to the physical thickness δ of the boundary layer and the universal function was obtained from experimental results on turbulent flat sheets in a compressible fluid.

One can thus support the hypothesis with a very simple argument based on the existence of a deficient velocity law according to which $\frac{u \cdot u_e}{u_\tau}$ is a function of $\frac{y}{\delta}$ independent of the abscissa. With the exception of the viscous sub-layer, friction is made up primarily of the turbulence term, and the classical concept of mixing length can be written in the form

$$\left(\frac{\tau}{\tau_p}\right)^{1/2} = \frac{l}{\delta} \frac{\partial\left(\frac{u_e - u}{u_\tau}\right)}{\partial\left(\frac{y}{\delta}\right)}.$$

The assumption of a universal function $\frac{l}{\delta}\left(\frac{y}{\delta}\right)$ rests on the admission that distribution $\frac{\tau}{\tau_p}\left(\frac{y}{\delta}\right)$ is itself independent of the abscissa in the case of a flat plate; this is a very probable assumption in view of the conditions with simple limits which affect τ/τ_p, and in view of experimental data.

A simultaneous examination of the experimental distribution of friction and velocity in a flat plate boundary layer allowed us to determine the given mixing length curve (Figure 1), which can be shown by the formula

$$\boxed{\frac{l}{\delta}=0{,}085\,th\left(\frac{k}{0{,}085}\,\frac{y}{\delta}\right)} \qquad \text{(II.3)}$$

The slope at the origin is k, which in accordance with most recent hypotheses was taken as:

$$k=0{,}41 \qquad \text{(II.4)}$$

Mixing length later diverges from this slope and tends toward a value of 0.085 in the outer part of the boundary layer.

II.1.3 Viscous sub-layer correcting function

Since the function F^2 for the viscous sub-layer is to be used to define turbulent friction between the wall, where its value is zero, and the turbulent zone, where its expression should approach the classical formula for mixing length, it was obtained by using the results of joining the linear velocity law in the laminar film and the turbulent logarithmic law for the wall (see Figure 2). A formula which is often used is that proposed by van Driest [3] to represent the experimental results of the case of cylindrical channel; it gives the velocity gradient by the formula:

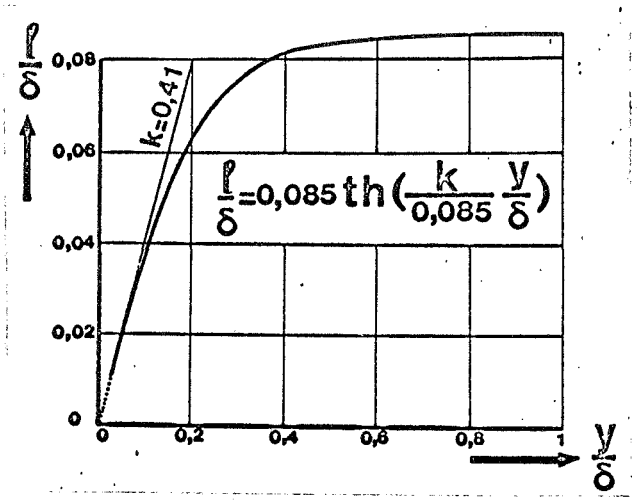

Figure 1. Universal curve for mixing length.

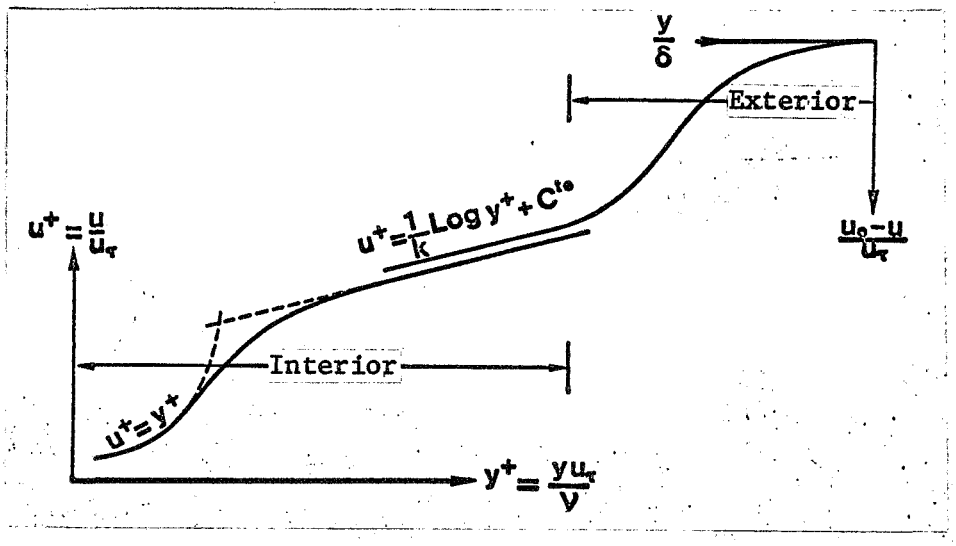

Figure 2. Functional diagram.

$$\frac{\partial u^+}{\partial y^+} = \frac{2}{1+\{1+4k^2y^{+2}(1-exp(-y^+/26))^2\}^{1/2}}; \qquad \text{(II.5)}$$

This law joins a linear law with a logarithmic one when y^+ goes from 0 to a higher value; the usual variables of the wall law are used:

$$u^+ = \frac{u}{u_\tau}\ ; y^+ = \frac{u_\tau y}{\nu}$$

where u_τ is the friction speed.

Since we are dealing with the vicinity of the wall, we can use the "wall approximation" in the classical manner, according to which the inertial forces are negligible compared to viscous and turbulent stress, so friction remains essentially equal to its value at the wall. We may also concede that mixing length is proportional to the distance to the wall. The Equation (II.2) proposed for total friction thus gives: /9

$$\frac{\tau}{\tau_p} = 1 = \frac{\partial u^+}{\partial y^+} + F^2 k^2 y^{+2} \left(\frac{\partial u^+}{\partial y^+}\right)^2. \qquad \text{(II.6)}$$

The solution of the system of Equations (II.5) and (II.6) immediately gives the desired elements. Laminar and turbulent friction, as well as the corrective function for the viscous sub-layer are thus given by the equations:

$$\frac{\tau_l}{\tau_p} = \frac{\partial u^+}{\partial y^+}, \qquad \text{(II.7a)}$$

$$\frac{\tau_t}{\tau_p} = \left(1-exp\left(-\frac{y^+}{26}\right)\right)^2 k^2 y^{+2} \left(\frac{\partial u^+}{\partial y^+}\right)^2, \qquad \text{(II.7b)}$$

$$F = 1 - exp\left(-\frac{y^+}{26}\right), \qquad \text{(II.7c)}$$

functions of y^+ in the case of a cylindrical channel or a flat plate under consideration.

It will also be necessary, however, to deal with other cases which may involve a fluid transfer at the wall or a compressibility effect where it does not appear probable that F^2 will still be a function of y^+. Thus, for a general case, we sought to make a hypotheses for F^2 which will include the parameters of viscosity and turbulence which might affect the phenomenon. For that we must assume that the corrective function in the general case is a universal function not of the distance to the wall, but of the ratio of turbulent friction to viscous friction τ_t / τ_l. This function is immediately derived from the elements just established for the flat plate which give:

$$2\frac{\tau_t}{\tau_l} = \left\{1 + 4\left(26\,kF\log_e(1-F)\right)^2\right\}^{1/2} - 1 \,. \qquad \text{(II.8)}$$

It may be more convenient to use the relation between the corrective function F^2 and the new ratio:

$$\frac{\tau_{t1}}{\tau_l} = \frac{1}{F^2}\frac{\tau_t}{\tau_l} = \frac{\rho l^2}{\mu}\frac{\partial u}{\partial y} \,.$$

The corresponding curve is shown in Figure 3. It shows that the corrective function F^2 is in fact zero when turbulent friction is zero, i.e., at the wall; it tends toward 1 when τ_{t_1} / τ_l tends toward infinity. It reaches in actuality a value very close to unity when the ratio of turbulent friction to viscous friction attains a value on the order of 40 or 50.

One can also see that the equation for total friction $\tau = \tau_l + \tau_t$, with /10
$\tau_l = \mu\frac{\partial u}{\partial y}$ and $\tau_t = \rho F^2 l^2\left(\frac{\partial u}{\partial y}\right)^2$ can be put in the form:

$$\frac{\tau \rho l^2}{\mu^2} = \frac{1}{F^2}\frac{\tau_t}{\tau_l} + \left(\frac{\tau_t}{\tau_l}\right)^2$$

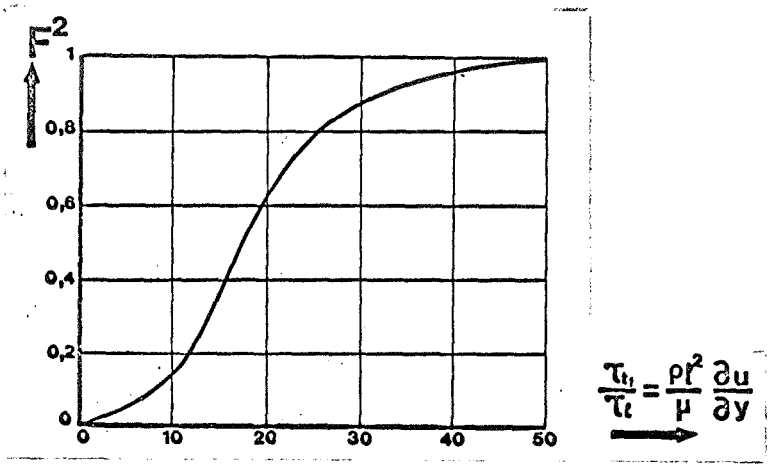

Figure 3. Corrective function for viscous sub-layer.

where:

$$2\frac{\tau_t}{\tau_l} = \left\{1 + \frac{4F^2\tau\rho l^2}{\mu^2}\right\}^{1/2} - 1.$$

Identifying it with (II.8), F is expressed as a function of total friction and mixing length by the following Formula (II.8 a)

$$F = 1 - \exp.\left\{-\frac{l}{26k\mu}(\tau\rho)^{1/2}\right\} \qquad \text{(II.8a)}$$

II.2. Research Principle for Equilibrium Boundary Layers

II.2.1 Preliminary Observations

The obvious interest of the hypotheses we have just set up is that they allow us to handle an expression for total friction in the different regions distinguished in the turbulent boundary layer and to use that expression to study local equations for the boundary layer.

It should be especially noted that the corrective function F^2 allows us to take up the viscous sub-layer; it can be used later to solve the equations for the boundary layer in the natural condition of u = o and y = 0.

In a general manner, it is possible to introduce the expression derived for friction in a local equation for momentum and attempt to solve it by numerical means; a finite differences technique currently under investigation should allow us thus to obtain exact results for all conditions at the boundaries which we might encounter.

Nonetheless, we attempted to find in advance a means of checking the hypotheses by applying them to a special, but important type of flow, i.e., that of equilibrium boundary layers. Moreover, it is in connection with these /11
equilibrium boundary layers, which represent the homolog of similar laminar solutions in the turbulent case, that we will be able to examine in a systematic manner the effect of such factors as pressure gradients and fluid transfer at the wall and to undertake an analysis of the effects of compressibility.

The general principle of this research uses the very classical notions of exterior and interior boundary layers in the majority of studies conducted so far on the turbulent boundary layer. The obvious interest in this technique is that it allows us to deal separately with the region in which viscosity occurs by taking advantage of a considerable simplification due to the proximity of the wall.

Nonetheless, we should emphasize that this simplification comes into play on the condition that the Reynolds number is large, because the hypothetical existence of an equilibrium boundary layer is not acceptable except in this case as will be seen later.

II.2.2 Example of an Impermeable, Incompressible Wall

a) Interior and exterior regions — overlapping condition

— According to ordinary concepts, the interior region is the region near the wall in which the forces of inertia are small compared to the viscous and turbulent friction terms and in which phenomena are essentially dependent on friction at the wall. Dimensional analysis leads us to represent the distribution of velocities in the form

$$u^+ = \frac{u}{u_\tau} = \text{function of } y^+ = \frac{u_\tau y}{\nu}$$

where u_τ is the friction speed:

$$\left(\frac{\tau_p}{\rho}\right)^{1/2}.$$

That is the wall law dealing with the viscous sub-layer where the corrective function F^2 comes into play and the turbulent wall region with logarithmic distribution.

— The exterior boundary layer, beginning at short distances y, is the region where the forces of inertia and friction are the same size; dimensional analysis leads us to represent variation in deficient velocity in the form:

$$\frac{(u_e - u)}{u_\tau} = \text{function of } \frac{y}{\delta}$$

a function which should be independent of the abscissa for equilibrium boundary layers.

— An important condition is that there may not be a discontinuity between the wall law and the deficient velocity law; in fact, the two overlap over one entire portion of the boundary layer; one very generally granted consequence is that the wall law and the deficient velocity law must both be in logarithmic form in the overlapping region.

b) Form of the wall friction law

The overlapping condition leads immediately to the expression of the friction coefficient of the wall as a function of the Reynolds number. In the overlapping region, the wall law and the deficient velocity law should be written: /12

$$\frac{u}{u_\tau} = \frac{1}{k} \log_e\left(\frac{u_\tau\, y}{\nu}\right) + C_1$$

$$\frac{u_e - u}{u_\tau} = -\frac{1}{k} \log_e\left(\frac{y}{\delta}\right) + C_2$$

Eliminating u/u_τ, we obtain:

$$\frac{u_e}{u_\tau} = \frac{1}{k} \log_e\left(\frac{u_\tau\, \delta}{\nu}\right) + C_1 + C_2 \qquad \text{(II.9a)}$$

or:

$$\sqrt{\frac{2}{C_f}} = \frac{1}{k} \log_e\left(\sqrt{\frac{C_f}{2}}\, \mathcal{R}_\delta\right) + C_{te} \qquad \text{(II.9b)}$$

This relationship, in which the friction coefficient is first expressed as a function of the Reynolds number for the physical thickness δ of the boundary

layer, is one of the basic relationships in our treatment of equilibrium boundary layers.

c) Universality of the wall law — Wall condition

It is admitted very generally that the logarithmic turbulent wall law is a universal relationship, which holds in the case of an impermeable wall when there is a pressure gradient dp/dx. It is useful to support this hypothesis and to show at the same time that it assumes that the Reynolds number is high enough.

Therefore, the "wall condition" will refer to the simplified boundary layer equation to be used in the vicinity of the wall and in which the inertia terms will be neglected. For an impermeable wall in an incompressible environment the Navier-Reynolds equation gives:

$$\left(\frac{\partial \tau}{\partial y}\right)_0 = \frac{dp}{dx} \quad \text{whence} \quad \tau = \tau_p + \frac{dp}{dx} y \,.$$

Using the variables of the wall law and deriving the parameter $\beta^x = \frac{\delta^x}{\tau_p} \frac{dp}{dx}$ for the equilibrium boundary layers, we may write:

$$\frac{\tau}{\tau_p} = 1 + \frac{\beta^x}{\frac{u_\tau \delta^x}{\nu}} y^+ \,. \qquad \text{(II.10)}$$

We see that the wall condition in its ordinary form $\tau = \tau_p$ is applicable to the case of pressure gradients, only if the Reynolds number tends toward infinity. The hypothesis to be proposed later will permit us to find the wall equation previously written for the flat plate with a pressure gradient:

$$1 = \frac{\partial u^+}{\partial y^+} + F^2 k^2 y^{+2} \left(\frac{\partial u^+}{\partial y^+}\right)^2 . \qquad \text{(II.6)}$$

The results established in paragraph II.1.3 thus hold for pressure gradients in the case of large Reynolds numbers. The universal wall law is thus the curve $u^+(y^+)$, which allowed us to accurately determine the corrective function F^2. With van Driests' Formula (II.5), where we let k = 0.41, we obtain the curve in Figure 4 which corresponds in the established turbulence to the logarithmic relationship:

$$\frac{u}{u_\tau} = \frac{1}{k} \log_e \left(\frac{u_\tau y}{\nu} \right) + 5{,}25 \qquad \text{(II.11)}$$

II.2.3. Extension to the General Case /13

Variables used — The preceding discussion may be taken up again in a more general case, i.e., for the study of fluid transfer at the wall and for the study of compressibiliy.

Interior and exterior regions, as well as a wall law and a deficiency law, are still defined and will be applied similarly to variables other than velocity (or to transformed variables). We still find that the variables in question should give way to logarithmic relationships in an area of overlapping and this condition dictates the technique which allows us to define them:

— in a study of the wall law the variable $\psi^+(u \text{ ou } h, \tau_p, \phi_p, \nu_p, \rho, \mu)$ is the first value sought which will give a logarithmic relationship for the established turbulence in the form:

$$\psi^+ = \frac{1}{k} \log_e \left(\frac{\rho_p u_\tau y}{\mu_p} \right) + C_1 \qquad \text{(II.12)}$$

— the corresponding deficiency variable should be $\psi_e^+ - \psi^+$ which, in the overlapping region, takes the logarithmic form

$$\psi_e^+ - \psi^+ = -\frac{1}{k} \log_e \left(\frac{y}{\delta} \right) + C_2 . \qquad \text{(II.13)}$$

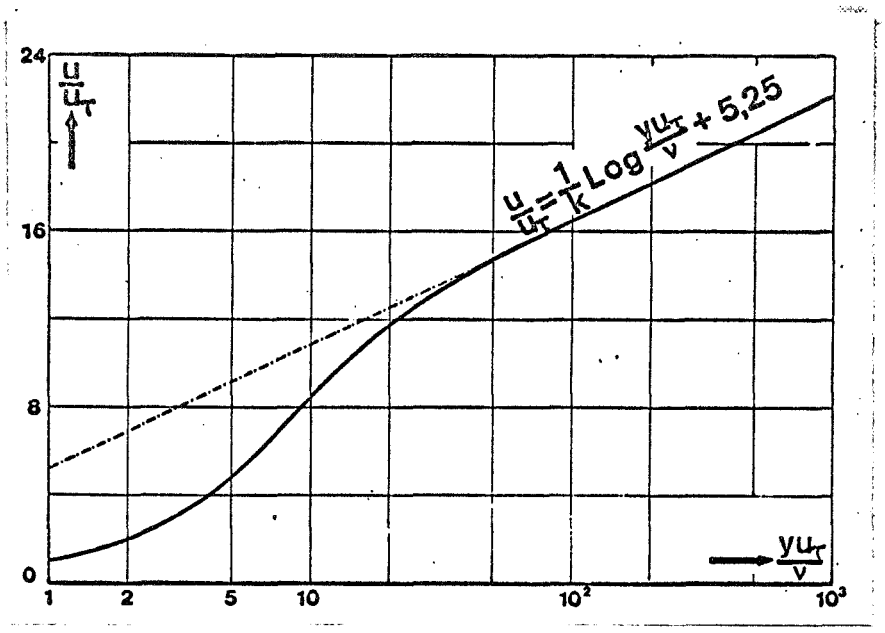

Figure 4. Incompressible wall law.

Laws of friction and fluid transfer at the wall — They are determined by eliminating Ψ^+ from (II.12) and (II.13) to give the logarithmic relationship:

$$\psi_e^+ = \frac{1}{k} \log\left(\frac{\rho_e u_\tau \delta}{\mu_p}\right) + C_1 + C_2 \qquad \text{(II.14)}$$

Wall conditions — We still seek the solution at sufficiently high Reynolds numbers so that the pressure forces are negligible compared to viscous and turbulent stress in the wall region.

In the case of fluid transfer at the wall, it will be necessary to keep /14 the inertia term because of the injection velocity. In a study to be made in an incompressible fluid, the Navier-Reynolds equation for the vicinity of the wall will thus becomes:

$$\left(\frac{\partial \tau}{\partial y}\right)_0 = \left(\rho \nu \frac{\partial u}{\partial y}\right)_0 \quad \text{where } \tau = \tau_p + \rho_p v_p u. \qquad \text{(II.15)}$$

In a study of an impermeable wall in compressible fluid, the wall conditions found from the momentum equation and the energy equation are written respectively

$$\frac{\partial \tau}{\partial y} = 0 \quad \text{where} \quad \tau = Cte = \tau_p \tag{II.16a}$$

$$\frac{\partial (u\tau - \phi)}{\partial y} = 0 \qquad u\tau - \phi = Cte = -\phi_p \cdot \tag{II.16b}$$

III. BOUNDARY LAYERS WITH PRESSURE GRADIENTS INCOMPRESSIBLE FLUIDS

III.1. Definitions and General Assumptions

An equilibrium turbulent boundary layer is defined simply as a flow for which the deficient velocity profiles remain similar, i.e. for which the curve of $\frac{u_e - u}{u_\tau}$ as a function of y/δ is independent of the abscissa. It was experimental data which first showed the existence of such boundary layers. The most obvious case and the first one observed was that of the flat plate. Clauser [4] and Rotta [5] found that certain pressure gradients could give rise to equilibrium boundary layers. Other authors, such as Bradshaw and Ferris [6], Herring and Norbury [7], and Stratford [8] later established results confirming their existence in various pressure gradients, positive or negative.

Equilibrium boundary layers were also the subject of quite a number of analyses on the theoretical exploitation level. The establishment of solutions from equations for the boundary layer is a quite recent development, however. We note the solution established by Mellor and Gibson [9] from a scheme for eddy viscosity through a treatment quite similar to that presented here.

A first attempt to analyze the conditions for obtaining an equilibrium boundary layer can be carried out, as was done by Bradshaw, from the overall equation for momentum in the boundary layer:

$$\tau_p = \frac{d}{dx}\left(\rho u_e^2 \theta\right) - \delta^* \frac{dp}{dx}.$$

Equilibrium would prevail when the friction force and the pressure force contribute to the variation in momentum in a proportional way. /15

Thus, the classical parameter $\frac{\delta^*}{\tau_p}\frac{dp}{dx}$ appears, which should remain constant for an equilibrium turbulent boundary layer (in the same way as in similar

solutions for a laminar boundary layer). This result will be found again in the treatment to follow.

III.2. Exterior Boundary Layer - Solution for Equilibrium Boundary Layers

The general principle of research, as stated before, consisted in dealing separately with the interior region, where the effects of viscosity are confined, and the exterior boundary layer, in order to make use of the overlapping condition and end up with a law of wall friction.

However, we have seen that in the case of an impermeable wall in an incompressible fluid, the effect of the pressure gradient diappears at large Reynolds numbers. The curve given for the flat plate is thus the universal wall law, which in established turbulence in the overlapping region tends toward the logarithmic form:

$$\boxed{\frac{u}{u_\tau} = \frac{1}{k} \log_e \left(\frac{u_\tau y}{\nu}\right) + 5{,}25} \,. \qquad \text{(III.1)}$$

It remains for us to solve the problem of the exterior boundary layer, for which we shall seek a solution to the local equation for the boundary layer.

III.2.1. Differential for Deficient Velocity

The region under study is that of an established turbulent flow where friction, composed primarily of the turbulence term, is expressed by the classical formula for mixing length:

$$\tau = \tau_t = \rho \ell^2 \left(\frac{\partial u}{\partial y}\right)^2$$

According to the hypothesis of our scheme, the evolution of mixing length is represented by the relationship:

$$\frac{l}{\delta} = 0{,}085\, th\left(\frac{k}{0{,}085}\,\frac{y}{\delta}\right)$$

where the scale is represented by the physical thickness δ of the boundary layer.

The thickness δ is also the distance to the wall one should refer to in this treatment. Thus, the dependent and independent variables are:

$$\boxed{\eta = \frac{y}{\delta}} \; ; \; \boxed{\frac{u_e - u}{u_\tau} = f'(\eta)} \qquad \text{(III.2)}$$

where f is differentiated with respect to η.

Then we hypothesize that the deficient velocity profile is invariable according to the abscissa, and: /16

$$\left(\frac{\partial f'}{\partial x}\right)_\eta = 0.$$

Finally, we use the hypotheses given above to express the different terms and develop the equation for momentum:

$$\rho u \frac{\partial u}{\partial x} + \rho v \frac{\partial u}{\partial y} = \frac{\partial \tau}{\partial y} + \rho u_e \frac{du_e}{dx} ,$$

bearing in mind the continuity equation.

Thus, we obtain a differential equation for f' as a function of η, an equation which is first written as:

$$\left(L^2 f''^2\right)' = -2\beta f' + \beta\gamma f'^2 - \beta \frac{u_e}{u_e'}\frac{\gamma'}{\gamma}\left(f' - \gamma f'^2 + \gamma f f''\right) + \beta\left(\frac{u_e}{u_e'}\frac{\delta'}{\delta} + 1\right)\left(\eta f'' - \gamma f f''\right). \qquad \text{(III.3)}$$

u_e', γ', δ' represent a derivative with respect to x, while f' and f'' indicate derivatives with respect to η. For greater clarity the following notations are used:

$$\gamma = \left(\frac{\tau_p}{\rho u_e^2}\right)^{1/2} ; \beta = -\frac{\delta}{\gamma u_e}\frac{du_e}{dx} ; L = \frac{\ell}{\delta} . \qquad \text{(III.4)}$$

The four equation parameters are:

$$\gamma, \frac{u_e}{u_e'}\frac{\gamma'}{\gamma}, \frac{u_e}{u_e'}\frac{\delta'}{\delta}, \beta .$$

An equilibrium solution can be really found to confirm the hypothesis only if these four parameters are constant.

In the first place, it is clear that this condition can be satisfied only if the friction term γ is zero. Thus, the equilibrium solution should correspond to a Reynolds number tending towards infinity. We next observe that the law of wall friction (II.9), which we will arrive at later through the overlapping condition, permits us to express the parameter:

$$\frac{u_e}{u_e'}\frac{\gamma'}{\gamma} ;$$

We have actually:

$$\frac{1}{\gamma} = \frac{1}{k}\log_e\left(\gamma\frac{u_e\delta}{\nu}\right) + Cte, \text{ d'où } : \beta\frac{\gamma'}{\gamma}\frac{u_e}{u_e'} = \frac{-\gamma/k}{1+\gamma/k}\beta\left(\frac{u_e}{u_e'}\frac{\delta'}{\delta}+1\right). \qquad \text{(III.5)}$$

Since it is on the order of γ, the parameter tends toward zero with it.

At large Reynolds numbers, Equation (III.3) is thus written:

$$\left(L^2 f''^2\right)' = -\beta\left(\frac{u_e \delta'}{u_e' \delta} + 1\right)\eta f'' + 2\beta f'. \tag{III.6}$$

/17

Now, in order to determine precisely the conditions, we shall first observe that the stream function f, following this equation, is defined only up to an approximate additive constant. To simplify, we shall select it so that:

$$f = 0 \text{ when } \eta = 0. \tag{III.7a}$$

Two further boundary conditions to be added are those of zero friction and zero deficient velocity at the edge of the boundary layer:

$$f_1' = f_1'' = 0 \text{ when } \eta = 1. \tag{III.7b}$$

Finally, the remaining parameter $\frac{u_e \delta'}{u_e' \delta}$ can be expressed by Equation (III.6) integrated from 0 to 1 and requiring that it satisfy the condition

$$L^2 f''^2 \equiv \frac{\tau}{\tau_p} = 1 \text{ when } \eta = 0. \tag{III.7c}$$

Thus, we find the relationship:

$$-\beta\left(\frac{u_e \delta'}{u_e' \delta} + 1\right) = \frac{1}{f_1} + 2\beta \tag{III.8}$$

which expresses the last parameter as a function of β.

The differential equation giving the distribution of deficient velocities for a boundary layer with a pressure gradient in the case of high Reynolds numbers finally becomes

$$\boxed{\left(L^2 f''^2\right)' = 2\beta f' + \left(\frac{1}{f_1} + 2\beta\right)\eta f''}. \tag{III.9}$$

It brings into play the only pressure gradient parameter:

$$\boxed{\beta = -\frac{\delta}{\sqrt{\frac{C_f}{2}}} \frac{1}{u_e} \frac{du_e}{dx}} \quad . \tag{III.9b}$$

III.2.2. Principal Characteristics Provided by the Solution.

We first note that the pressure gradient parameter β, formed here with the physical thickness δ of the boundary layer, is directly linked to the parameter

$$\frac{\delta^*}{\tau_p} \frac{dp}{dx}$$

which is used more commonly in the study of equilibrium boundary layers. In effect, we have:

$$\beta = \frac{1}{f_1} \frac{\delta^*}{\tau_p} \frac{dp}{dx} \tag{III.10}$$

where f_1 is a function of β given by the solution of Equation (9).

A technique for the numerical solution of this equation has been developed and applied for a whole series of positive and negative values of the parameter β. The solution thus gives the family of deficient velocity profiles $f'(\eta)$ of the equilibrium boundary layers for negative and positive pressure gradients, the latter up to the separation point of $(\beta \to -\infty)$. It also provides the friction profiles $\frac{\tau}{\tau_p}\left(\frac{y}{\delta}\right)$. /18

Characteristic integral ratios can also be derived which are commonly used for the study or utilization of equilibrium boundary layers:

$$f_1 = \int_0^1 f' d\eta = \frac{\Delta}{\delta} \tag{III.11a}$$

$$f_2 = \int_0^1 f'^2 \, d\eta. \qquad \text{(III.11b)}$$

The first brings into play the Clauser thickness Δ.
The factor for the deficient velocity profile in its usual form is:

$$G = \frac{f_1}{f_2} \qquad \text{(III.12)}$$

f_1, f_2 and G are functions of the pressure gradient function β determined by the solution of Equation (III.9).

The asymptotic form of the equation used limits in principle the results to the region of very high Reynolds numbers. Experience, as well as attempted nonasymptotic solutions where γ is taken into account, show that the deformation of the deficiency profile is small and that asymptotic results can, in fact, be used in a wide range of Reynolds numbers to cover numerous practical problems.

It should be emphasized that the so-called "exterior" region overlaps the wall region up to very small y distances, a property which allows us to determine rather closely the common integral thicknesses of the boundary layer by integration from $y = 0$ of the deficiency profile. For displacement thicknesses and momentum, the following formulas are obtained:

$$\frac{\delta^*}{\delta} = f_1 \left(\frac{C_f}{2}\right)^{1/2}$$

$$\frac{\theta}{\delta} = f_1 \left(\frac{C_f}{2}\right)^{1/2} - f_2 \frac{C_f}{2}. \qquad \text{(III.13)}$$

III.2.3. Wall Friction Law.

The relationship for the coefficient of wall friction is found through the use of the overlapping of the wall law, given in the turbulent portion by the logarithmic Formula (III.1) and the law of deficient velocity given by the solution of Equation (III.9). The form of this equation and its solution show that at small values of η deficient velocity is given by the logarithmic relathionship to the first order:

$$\frac{u_e - u}{u_\tau} = -\frac{1}{k} \log_e \frac{y}{\delta} + D_V \qquad \text{(III.14)}$$

where D_V is a function of the pressure gradient parameter.

Eliminating u/u_τ from Equations (III.1) and (III.14) we find a relationship for the friction coefficient expressed as a function of thickness δ: /19

$$\left(\frac{2}{C_f}\right)^{1/2} = \frac{1}{k} \log_e \left(\mathcal{R}_\delta \left(\frac{C_f}{2}\right)^{1/2}\right) + D_\gamma \qquad \text{(III.15)}$$

with

$$D_\gamma = D_V + 5{,}25$$

The next step is to introduce the Reynolds number for the displacement thickness into the friction law, using Formula (III.13) for δ^*/δ. This gives the classical formula:

$$\boxed{\left(\frac{2}{C_f}\right)^{1/2} = \frac{1}{k} \log_e \mathcal{R}_{\delta^*} + D^*} \qquad \text{(III.16)}$$

with

$$\boxed{D^* = D_\gamma - \frac{1}{k} \log_e f_1}$$

/8 is also a function of β determined by the solution.

III.2.4. Limiting Cases of the Solution.

Lower limit with negative pressure gradient. Study of Equation (III.9) in the integrated form shows that the coefficient $1/f_1 + 2\beta$ should remain positive if friction is not to become negative at any point in the boundary layer. There is consequently a lower limiting value of the pressure gradient parameter in accelerated flow. Numerical solution gave this limit as:

$$\beta_{limit} = \frac{1}{2f_{1\,limit}} = -0{,}44 \quad et \quad \beta^*_{limit} = -0{,}5.$$

It will be shown later (paragraph III.4.2) that the coefficient $1/f_1 + 2\beta$ is proportional to the exterior fluid drawn away through the boundary layer. The physical significance of this limit is simply that this entrainment cannot be negative.

Large β results — Separation. The variable f' used becomes infinite at separation ($u_\tau = 0$), and in this case, it is interesting to replace it by a variable such as $\frac{u_e - u}{u_\tau \beta}$ which remains finite. The solution for separation must be determined in principle from the form of the deficiency equation with this new variable and when β tends toward infinity.

Here, we shall confine ourselves to observing that $\frac{u_e - u}{u_\tau \beta}$ varies very slowly with β at large values. Distributions corresponding to the values given below for β = 2 and β = 5 are almost identical and should appreciably represent the separation profile.

Similarly, the ratios of the different parameters to β vary very slowly and may be extrapolated closely up to $1/\beta = 0$. The values to be retained in separation are:

$$\frac{f_1}{\beta} = 15 \; ; \; \frac{G}{\beta} = 24{,}7 \; ; \; \frac{D^x}{\beta} = 42{,}9. \qquad \text{(III.17)}$$

Note in conclusion that the velocity profile is easily found from the separation and the form parameter corresponding to it: the law of friction (III.16) gives the following when C_f tends toward 0 at a finite $\mathcal{R}_{\delta^*}$: /20

$$D^*\left(\frac{C_f}{2}\right)^{1/2}=1 \text{ when } G\left(\frac{C_f}{2}\right)^{1/2}=0{,}575 \text{ and } \frac{\delta^*}{\theta}=2{,}35. \tag{III.18}$$

III.3. Presentation of Equilibrium Boundary Layer Results

III.3.1. Principal Results of the Solution

A numerical program utilizing a simple difference technique with narrow intervals (more than 400 steps from $\eta = 1$ to $\eta = 0$) was applied to the resolution of equation (III.9) with many values of the pressure gradient parameter from the lower limit $\beta = -0.44$ to a high positive value corresponding to conditions very close to those of separation(1).

Table 1 gives the numerical values for deficient velocity f' as a function of η for some of the parameters of pressure gradient β.

It is completed by Table II where we have regrouped the different constants and integral characteristics of the equilibrium profile as functions of β.

Figure 5 shows the deficient velocity profiles. Using a logarithmic scale for η we find the curves to be linear at small values of η with a slope of $1/k$. The profiles for large values of β are shown as explained by using the variable f'/β; one should note the very slow variation pointed out previously and the tendency toward a limiting curve which should correspond to the separation profile.

(1) In numerical calculation a modified variable was used for f in order to eliminate an iteration previously used until the boundary conditions were satisfied. The results obtained are slightly different from from those presented at Stanford [1].

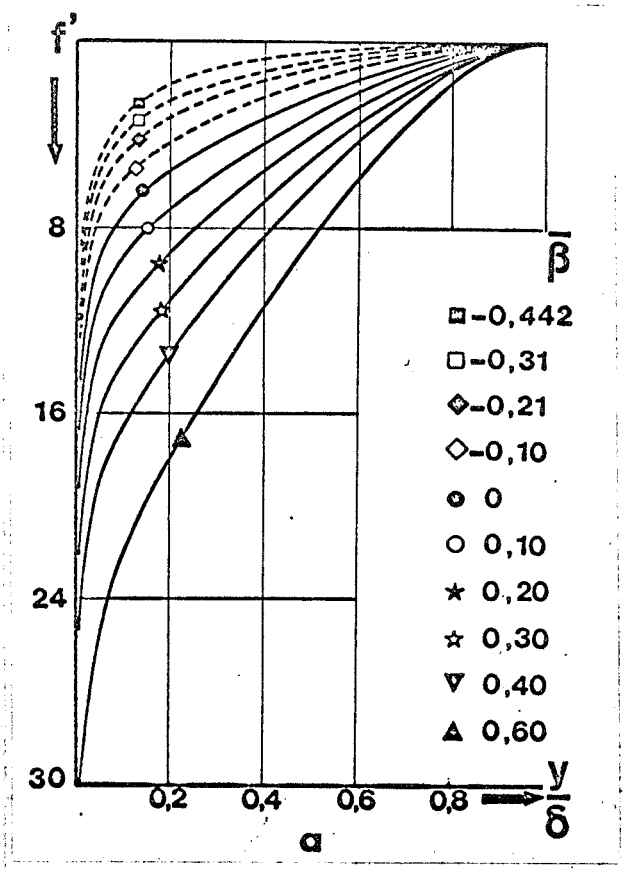

Table 1.

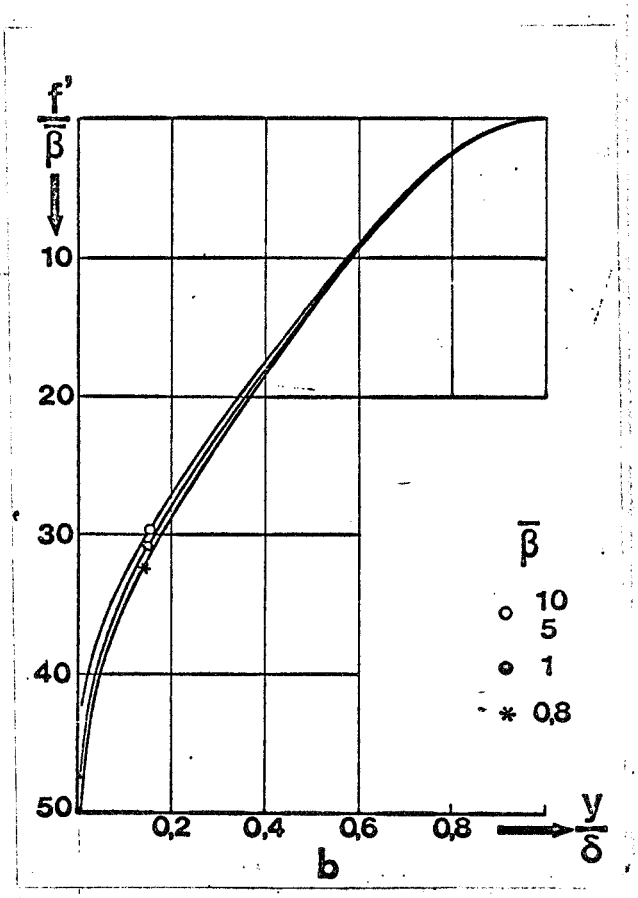

Table 2.

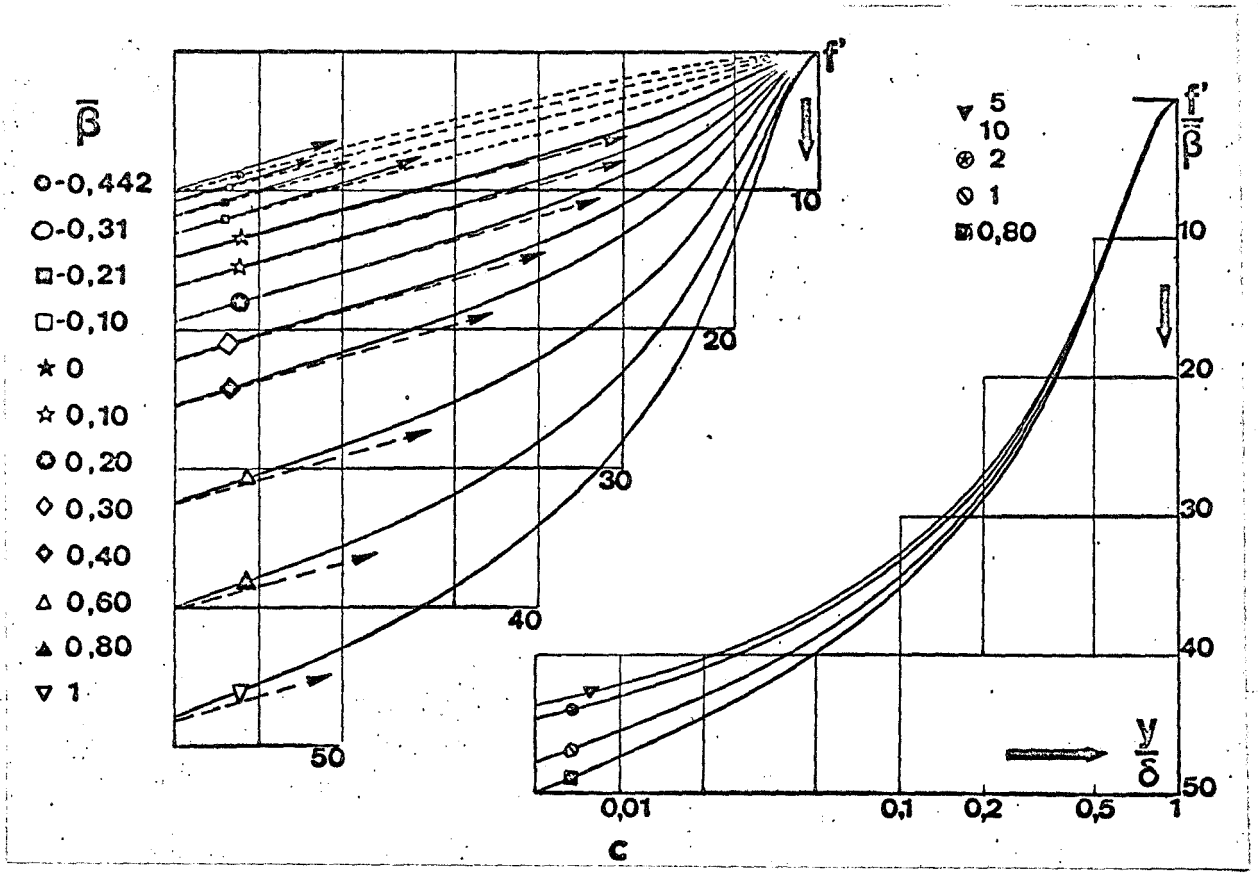

Figure 5. a) Deficient velocities; b) Deficient velocities with large $\bar{\beta}$; c) Deficient velocity profiles. Logarithmic scale for y/δ.

Figure 6 shows friction distributions $\left(\frac{\tau}{\tau_p} = L^2 f''^2\right)$ in the boundary layer. One should note in particular the effect of positive pressure gradients which quickly give rise to a maximal friction much greater than the wall friction. At large values of β representation in the form $\tau/\tau_p \beta^2$ leads to curves which vary very little and whose limit gives the friction profile for separation.

Figure 7 shows the evolution of the wall friction coefficient with the Reynolds number for displacement thickness $\delta^{(1)}$ (Formula III.16). We see that negative pressure gradients give rise to an increase in C_f which is normal and that positive gradients produce the opposite effect, giving zero friction when β tends toward infinity.

III.3.2. Comparison With Experimental Data.

One interesting aspect of studies in incompressible fluids is that we can check the scheme hypotheses by comparison with a great number of confirmed experimental data. Such checks were carried out in particular on the occasion of the Stanford conference, for which an important preparatory project by Coles and Hirst [2] provided a considerable volume of experimental data. This document was widely used for our comparisons regarding deficiency velocity profiles. In order to avoid the experimental inaccuracy which is almost inevitable in determination of physical thickness δ, we preferred always to relate the distance y to Clauser's thickness integral:

$$\Delta = \int_0^\delta \frac{u_e - u}{u_\tau} dy.$$

The first comparison of our solution with experimental results (Figure 8) deals with the case of a flat plate. The experimental results are those which gave rise to the well-known regrouping carried out by Clauser [4]. Obviously, we expected satisfactory agreement since it is from these very velocity and friction distributions in a boundary layer of a flat plate that our hypothesis on mixing length was established.

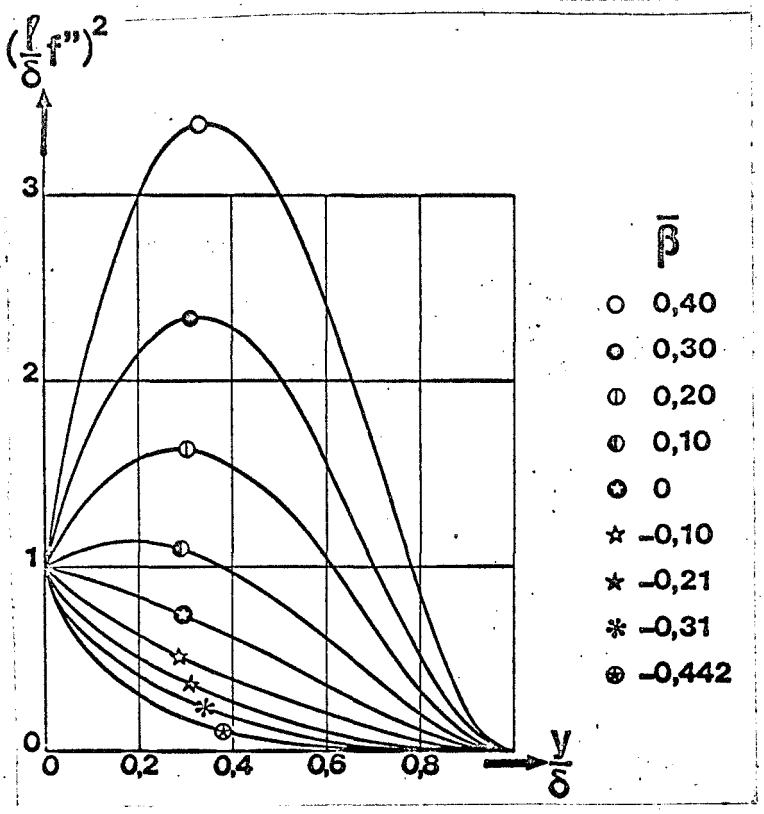

Figure 6.

a) Friction profiles

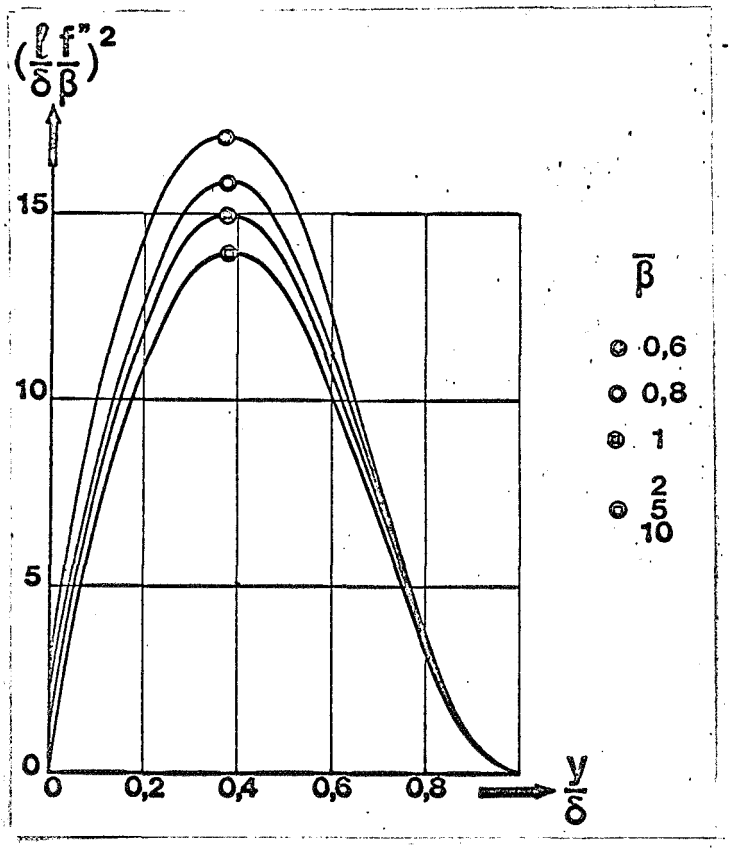

Figure 6.

b) Friction profiles with large $\bar{\beta}$.

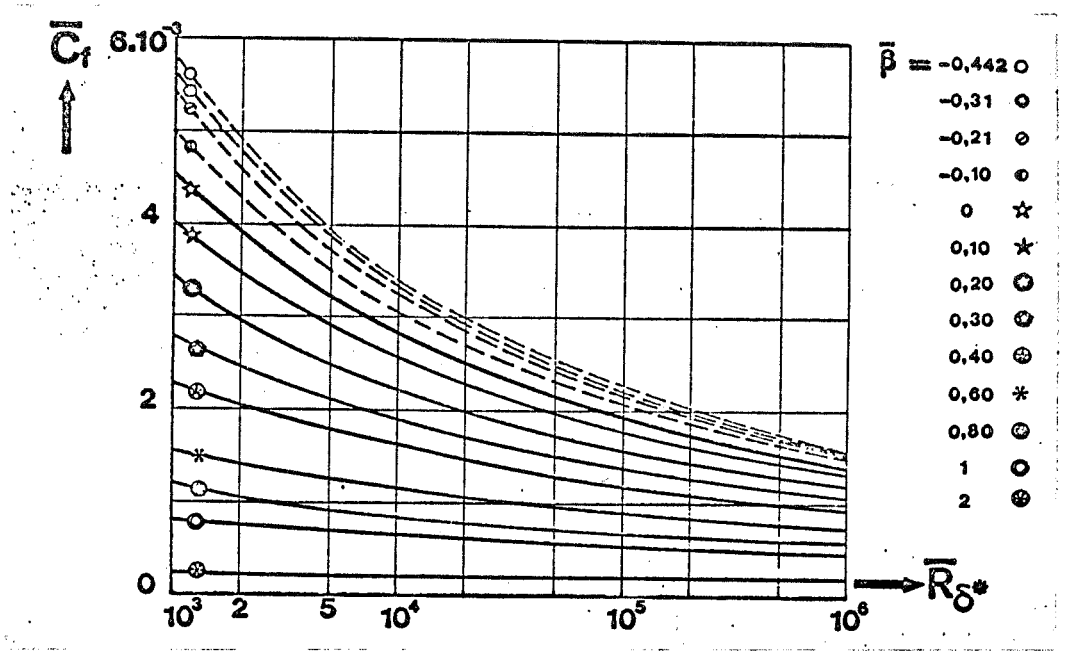

Figure 7. Evolution of the friction law with $\bar{\beta}$.

$$\frac{1}{(\frac{\bar{C}_f}{2})^{1/2}} = \frac{1}{k}\text{Log}\bar{R}_{\delta^*} + D^*$$

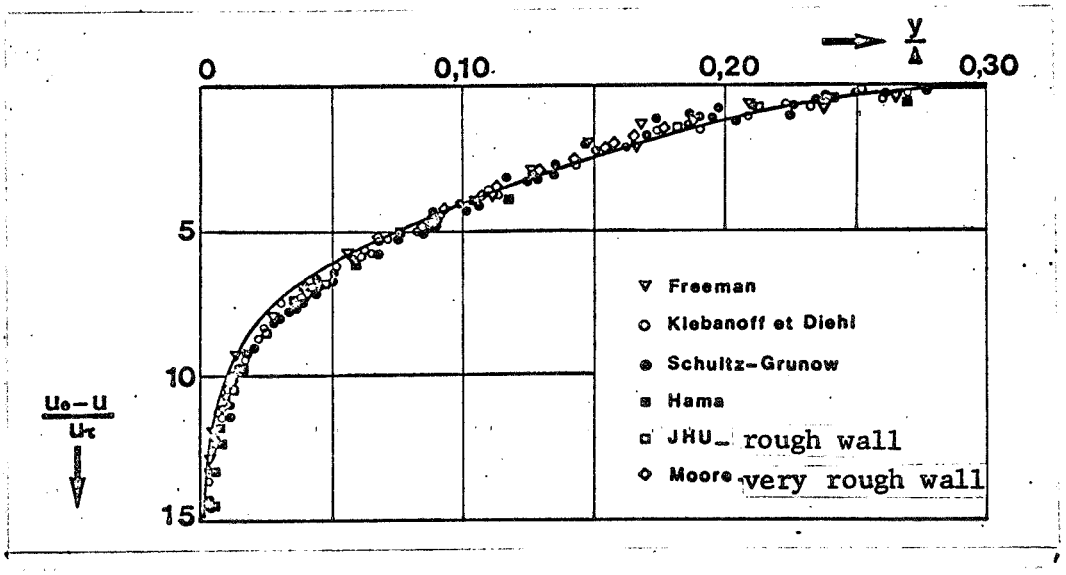

Figure 8. Comparison with the experimental results for a flat sheet regrouped by Clauser.

The check involved comparing the solution with the majority of available /24
experimental results concerning equilibrium boundary layers with pressure gradients — results which were reanalyzed as a whole in great detail by Coles and Hirst. Note that the object was not to compare experimental results with a calculation of the boundary layer but to check that the experimental profiles could be effectively shown by the proposed family of theoretical profiles. Each comparison was performed with the theoretical profile chosen in each case as that which corresponds to the experimental value of the factor in the form of G. The results obtained are shown in Figures 9a through 9d.

— Figure 9 shows the results obtained by Herring and Norbury [7] which involve a negative pressure gradient.

— Figures 9b and 9c show the experimental results of Bradshaw and Ferris /25
[6] and Clauser [4] found with positive gradients.

— Figure 9d shows the comparison with velocity profiles measured by Stratford [8] in conditions near separation.

Finally, Figure 10 gives the comparison with experimental profiles plotted by Schubauer and Klebanoff [10] with different abscissas in a pressure gradient up to separation of the boundary layer. We are no longer dealing with an equilibrium boundary layer, as the considerable variation of the form factor G shows. It is obviously of interest to observe that the experimental profiles can still be represented by those of the family of equilibrium profiles.

A noticeable divergence between the experimental profiles and the equilibrium profiles occurred only in the special case of relaxing flows — thus, for example, a flow in which an intense positive pressure gradient leads to conditions close to separation and which is later attenuated and returns to a uniform flow. We were able to note that the profiles plotted with respect to the maximum form-parameter could be quite noticeably different from an equilibrium profile when it increases toward a flat plate value with the same form factor G.

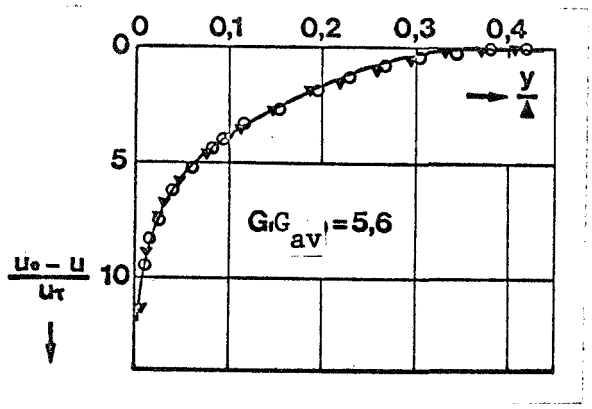

Figure 9a. Comparison with the experimental results of Herring & Norbury ($\beta < 0$).

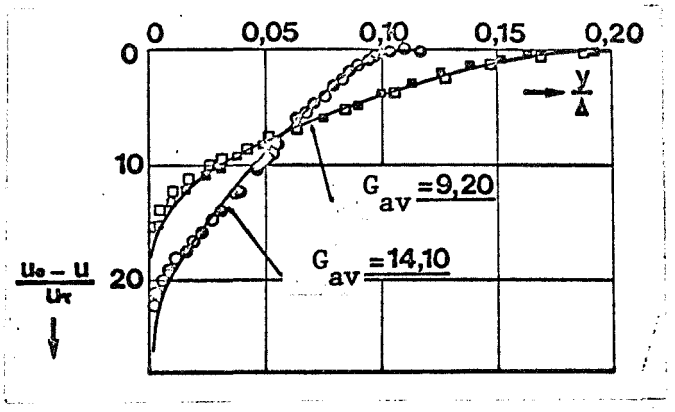

Figure 9b. Bradshaw's experimental profiles ($\beta > 0$).

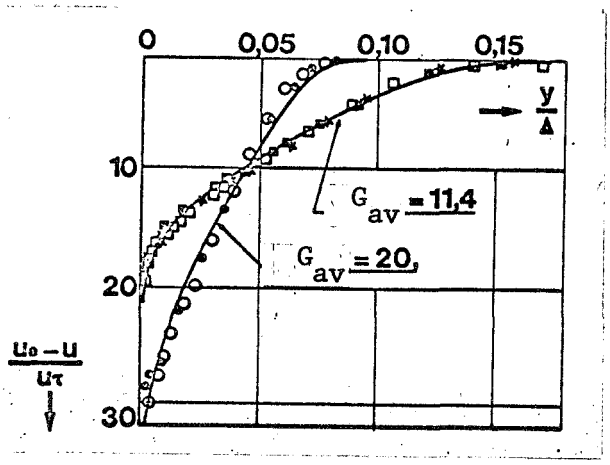

Figure 9c. Clauser's experimental profiles ($\beta > 0$).

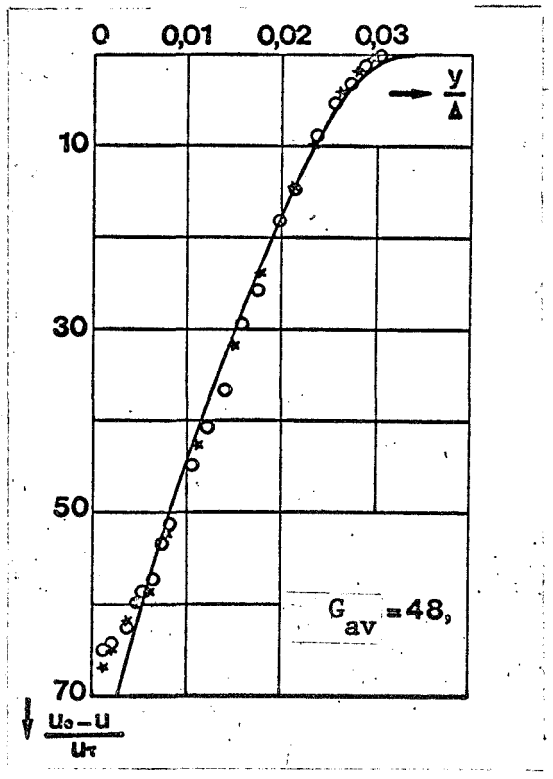

Figure 9d. Stratford's separation profile.

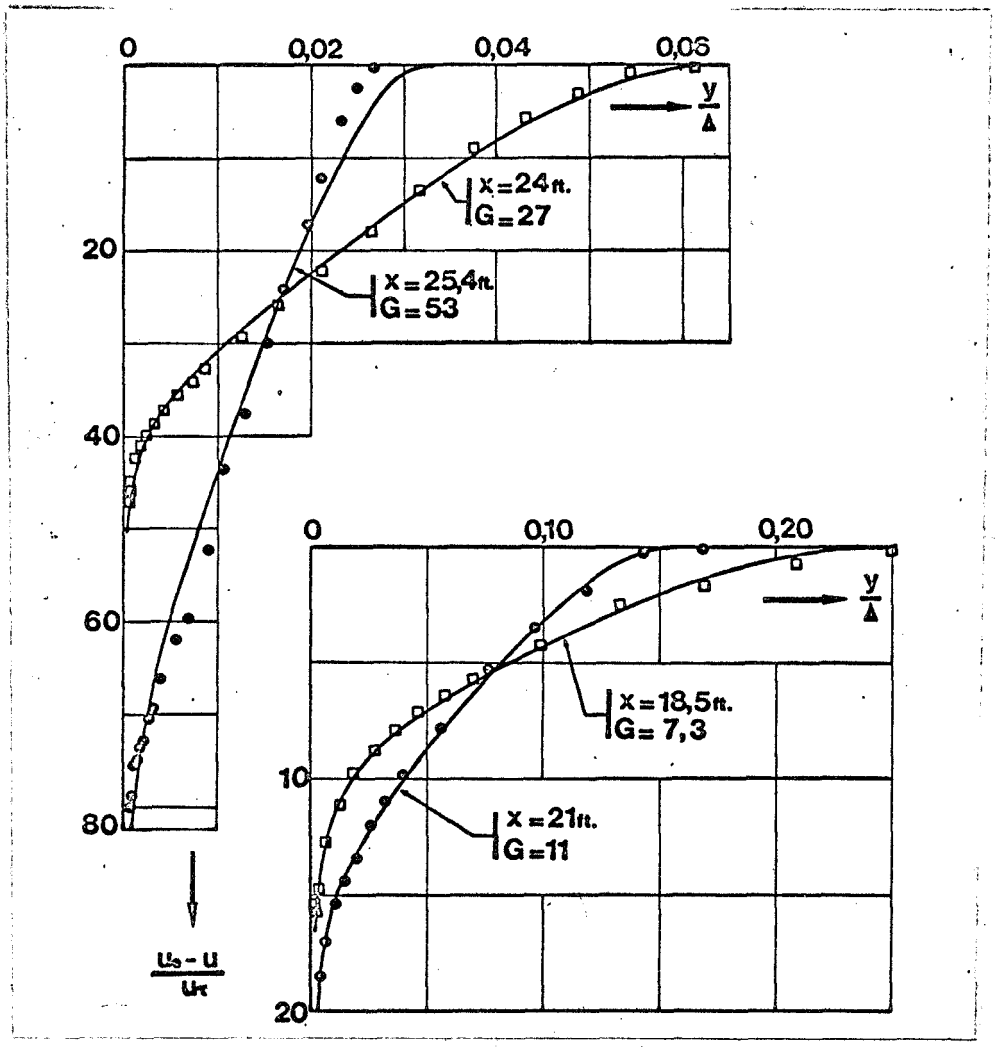

Figure 10. Comparison with the results of Schubauer and Klebanoff.

III.4. Utilization of an Integral Method of Calculation for the Case of a Nonequilibrium Boundary Layer /26

III.4.1. General Principle

In view of the preceding comparisons, we may seek to establish an approximative method of calculation for predicting the development of the boundary layer in the case of a flow with any given pressure gradient using the results relating to equilibrium boundary layers in solving the boundary layer global equations. Such a method was prepared and applied [1]; we shall review the technique and some of its results.

The most immediate technique, altogether comparable to that of the Karman-Polhausen method for laminar flow, would mean using related laws directly which relate the form parameter and the wall friction coefficient to the pressure gradient parameter β for an equilibrium boundary layer, in order to solve the global momentum equation.

However, experimental results show that if the velocity profiles can be correctly represented by the family of equilibrium profiles, the relationship between the form parameter and the experimental pressure gradient parameter β may differ considerably from that of an equilibrium boundary layer in the general case.

A better technique consists of joining an auxiliary global equation to the Karman equation, bringing into play the characteristic parameters of equilibrium profiles but without direct use of β. The auxiliary equation used here is the entrainment equation.

III.4.2. Equations and Solution Method

Karman equation. The general form of the overall equation for momentum in an incompressible plane flow is:

$$\frac{C_f}{2} = \frac{d\theta}{dx} + \theta \frac{\delta^*/\theta + 2}{u_e} \frac{du_e}{dx} - \frac{1}{u_e^2} \frac{d}{dx} \int_0^\delta \left(\overline{u'^2} - \overline{v'^2}\right) dy \qquad \text{(III.19)}$$

The term including the longitudinal derivatives of turbulence intensity is neglected in the quasi-totality of calculating methods proposed so far. Given, however, that it can play an important part in intense pressure gradients, especially approaching separation, we deemed it necessary to retain it and look for an estimate of its value.

This estimate is found very easily by returning to the elementary hypothesis of the mixing length theory, according to which fluctuations u' and v' are proportional to each other over the greater part of the boundary layer. The appropriate term in the Karman equation is thus in the form:

$$\int_0^\delta \left(\overline{u'^2} - \overline{v'^2}\right) dy = \frac{C}{\rho} \int_0^\delta \tau_t \, dy \,, \qquad \text{(III.20)}$$

where τ_t is turbulent friction and C is a constant to be found empirically.

Schubauer and Klebanoff's analysis of turbulence measurements bore out the preceding relationship and led to a constant C on the order of 3.5; this value was used in boundary layer calculations approaching separation.

Entrainment equation. Introduced initially in an empirical manner by Head [11], the entrainment equation can be justified and evaluated through the use, for instance, of the following arguments:

— The entrainment equation is made of none other than the overall continuity equation:

$$\frac{d\delta}{dx} - \frac{v_e}{u_e} = \frac{1}{u_e} \frac{d}{dx} \left[u_e (\delta - \delta^*)\right]. \qquad \text{(III.21)}$$

Empirically, Head found the entrainment $\frac{d\delta}{dx} - \frac{v_e}{u_e}$, by granting that it is a function of the form parameter $\delta \cdot \delta^*/\theta$, and resorting to experimental data to determine the function. We propose to replace this empirical approach by using the properties of equilibrium boundary layers. /27

— Let us first observe that at the edge of the boundary layer ($y = \delta$) the local momentum equation can be written:

$$\rho u_e \frac{du_e}{dx} - \rho u_e \frac{\partial u}{\delta y} \frac{d\delta}{dx} + \rho v_e \frac{\partial u}{\partial y} = \frac{\partial \tau}{\delta y} + \rho u_e \frac{du_e}{dx}.$$

Thus, entrainment is connected with the friction derivative by relationship to velocity:

$$\frac{d\delta}{dx} - \frac{v_e}{u_e} = -\frac{1}{\rho u_e} \left(\frac{\delta \tau}{\partial u}\right)_{y=\delta}.$$

— Given the fact that the hypothesis was made from a family of equilibrium profiles, we can find the friction derivative by means of Equation (III.9) for equilibrium boundary layers; this immediately gives for $\eta = 1$:

$$\frac{\partial(\tau/\tau_p)}{\partial\left(\frac{u_e - u}{u_\tau}\right)} = \frac{1}{f_1} - 2\beta = P,$$

whence we can find the entrainment

$$\frac{d\delta}{dx} - \frac{v_e}{u_e} = P\sqrt{\frac{C_f}{2}} \qquad \text{(III.22)}$$

— The parameter $P = \frac{1}{f_1} + 2\beta$ thus appears to be the essential one by means of which the equilibrium layer results are incorporated into the integral method. We shall regard the other parameters f_1, G, D^* and T as functions of P and not of β; These functions, determined by the solution for the equilibrium boundary layers, are given by the numerical values in Table II.

Final system to solve and relationships used: The method consists of simultaneously solving the two overall equations:

— Karman equation; written in the form

$$\frac{C_f}{2} = \frac{d\theta}{dx} + \theta \frac{\delta^*/\theta + 2}{u_e} \frac{du_e}{dx} - \frac{C}{\rho u_e^2} \frac{d}{dx} (\delta \tau_p T)$$

with

$$T = \int_0^1 \left(\frac{\tau}{\tau_p}\right) d \frac{y}{\delta}$$

— entrainment equation; in view of the arguments, it becomes:

$$P \sqrt{\frac{C_f}{2}} = \frac{1}{u_e} \frac{d}{dx} \left[u_e (\delta - \delta^*)\right]$$

— the integral thickness ratio is found from the formulas:

$$\frac{\delta^*}{\delta} = f_1 \sqrt{\frac{C_f}{2}} \qquad \frac{\theta}{\delta^*} = 1 - G \sqrt{\frac{C_f}{2}}$$

— the relationship for the friction coefficient is:

$$\sqrt{\frac{2}{C_f}} = \frac{1}{k} \log \frac{u_e \delta^*}{\nu} + D^*$$

— the solution for the equilibrium boundary layers gives the different parameters as functions of the entrainment parameter $P = \frac{1}{f_1} + 2\beta$ /28

$$f_1 = f_1(P)\,;\; G = G(P)\,;\; D^* = D^*(P)\,;\; T = T(P)$$

Their numerical values are given in Table II.

III.4.3. Sample Results

The method just presented was applied at the Stanford Conference to a whole series of experimental cases chosen by Coles and Hirst involving the consideration of a great variety of pressure gradients. Figure 11 shows four typical examples of results found from that method by comparing the calculated evolution for the form parameter δ^*/θ, the friction coefficient C_f, and the Reynolds number for momentum thickness $R_\theta = \frac{u_e \theta}{\nu}$ to experimental data.

We should note the completely satisfactory agreement found in the case of Herring and Norbury — that is to say, in an accelerated exterior flow.

Newman's experiments and those of Schubauer and Klebanoff relate to a positive pressure gradient intense enough to lead to separation of the boundary layer. We thus tried to keep in mind in the calculation the effect of the term including the longitudinal turbulence derivatives.

The best results were found for Newman's experiments: the use of a turbulent term constant C = 3.5 effectively improves the results, especially as regards the form parameter and R_θ, and the development of the boundary layer is correctly predicted practically up to separation.

On the other hand, in Schubauer and Klebanoff's case it is clear that taking into account the turbulence terms was not adequate to follow the development of the boundary layer up to separation, even with a constant C greater than 3.5. This is a case, in fact, where the vast majority of the calculation methods proposed at Stanford fell short of the mark. It would appear that the important effects of tridimensionality, due to the development of boundary layers on the side walls of the blower, were present in these experiments (as in many others). It is always quite difficult to distinguish the effects arising from the turbulence terms, and this is an almost insurmountable problem in real control of calculation methods through experimentation.

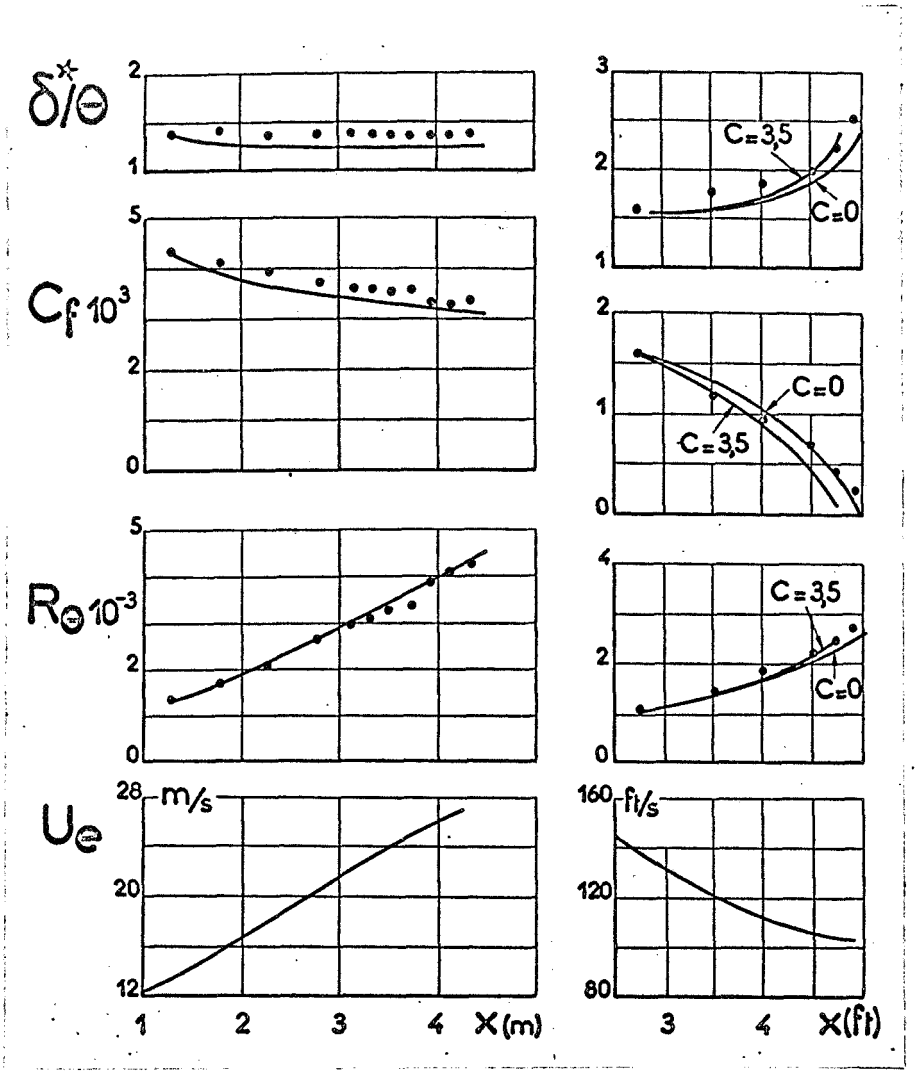

Herring and Norbury (ident. 2700)

Newman-Airfoil (ident. 3500)

Figure 11. Sample comparisons of integral calculation method and experimental results.

(Figure continued on next page)

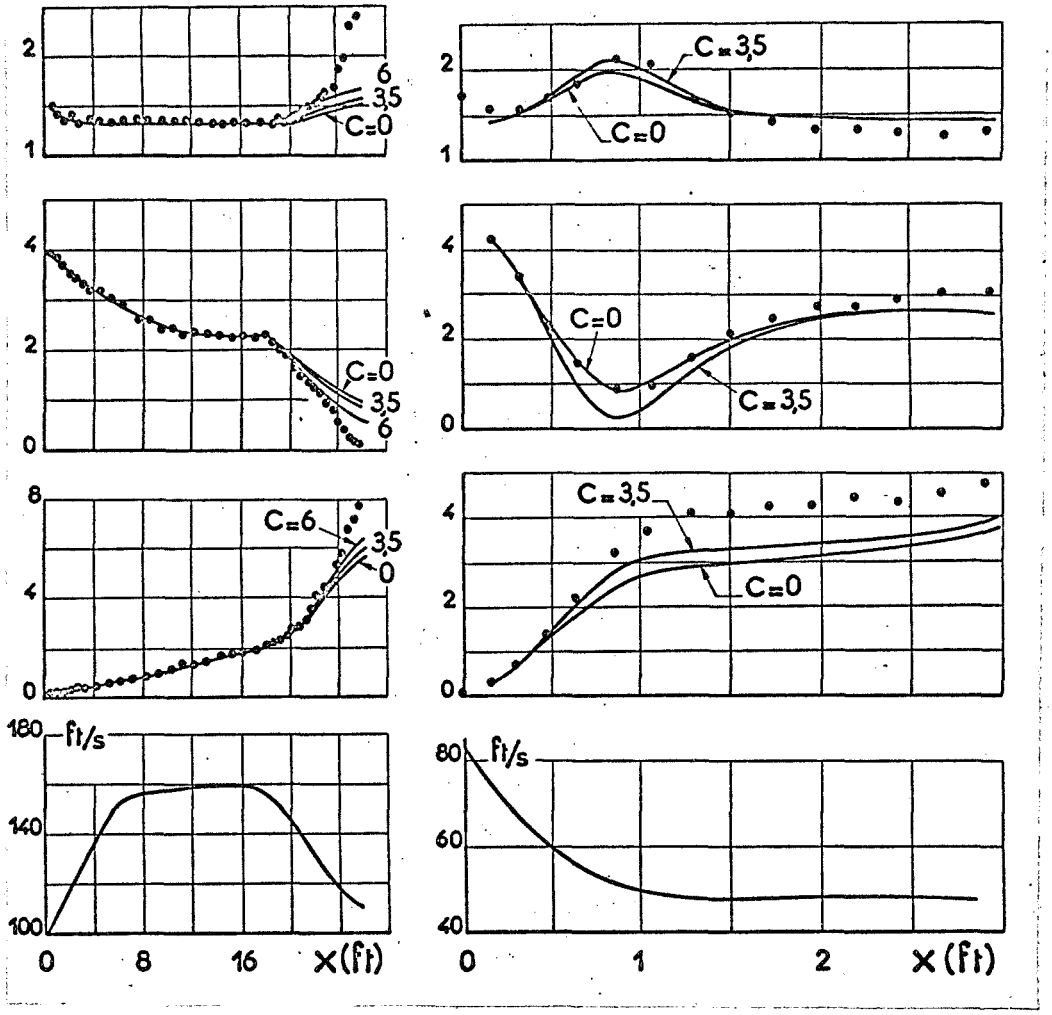

Schubauer and Klébanoff (ident. 2100)

Moses (ident. 4000)

Figure 11. Sample comparisons of integral calculus method and experimental results.

The "Moses" case refers to a "relaxing" flow; a strong positive pressure gradient leads up to the neighborhood of separation (H increases to 2.2 and C_f diminishes to almost zero); it is next attenuated to the extent that it gives uniform flow downstream. It is in this case that a difference between the experimental velocity profile and the theoretical equilibrium profile appears in the relaxation region following the minimum of the friction coefficient.

In spite of that, the calculated form parameter and friction are close enough to the experimental values; the deviation is more noticeable for the momentum thickness. It should be noted that we are dealing here with a boundary layer developing along a cylinder, and that the computation did not take into account the eventual effect of transverse curvature.

IV. CASE OF A FLUID TRANSFER AT THE WALL

/30

IV.1. Introduction - Review of Research Principle

Still in an incompressible fluid, we now propose to study the case of a fluid transfer to the wall, which differs from the impermeable case by the new limiting condition of a nonzero vertical velocity v_p which may be either positive (blowing) or negative (suction).

We still apply the technique of treating the interior and exterior regions separately in order to then use the necessary overlapping of the corresponding laws.

For the exterior region, we still hypothesize equilibrium, but in order to do so in developing the boundary layer equation it is necessary to first specify to which variable the equilibrium hypothesis should apply. The method is to use the overlapping condition and first to seek the variables ψ^+ and $\psi_e^+ - \psi^+$ which will give the logarithmic functions in the overlapping area. We shall find that the variables u^+ and $u_e^+ - u^+$ for the impermeable wall need to be replaced by the transformed variables V^+ and $V_e^+ - V^+$ to bring in the injection velocity:

$$V^+ = \frac{2}{v_p^+}\left\{(1+v_p^+ u^+)^{1/2} - 1\right\} \text{ with } v_p^+ = \frac{v_p}{u_\tau}. \tag{IV.1}$$

These are functions previously used in studies of the turbulent boundary layer with mass injection. We see that they were introduced so far primarily in analysis of experimental results, while now they will be used in a theoretical solution. We also see that the experimentation in question has so far been limited to the case of uniform exterior flow; we shall be able to establish theoretical results in the presence of pressure gradients just as we did for the impermeable wall.

We may further attempt a first analysis of the conditions which should be achieved to obtain an equilibrium boundary layer through the use of the overall momentum equation which is now written:

$$\tau_p + \rho v_p u_e + \delta^* \frac{dp}{dx} = \frac{d}{dx}(\rho u_e^2 \theta). \qquad \text{(IV.2)}$$

There would thus be equilibrium when the forces of pressure, friction and momentum $\rho v_p u_e$ due to mass injection contribute proportionally to the variation in momentum in the boundary layer. This condition introduces two parameters:

$$P = \frac{\rho v_p u_e}{\tau_p} \quad \text{and} \quad \frac{\delta^*}{\tau_p + \rho v_p u_e} \frac{dp}{dx}.$$

We shall find that an equilibrium solution in the development can be found if we assume that P is constant; we shall see a transformed pressure gradient parameter emerges which brings $\tau_p + \rho v_p u_e$ in place of the τ_p in the impermeable case.

IV.2. Interior Region - Wall Law

/31

IV.2.1. Wall Equation

It is quite obvious that the new condition $v_p \neq 0$ does not allow us to use a universal wall law $u^+(y^+)$ as in the impermeable case, and we must find the modifications that fluid transfer brings about in the distribution of velocities in the interior region. It is here that the hypotheses concerning mixing length and the corrective function for the viscous sub-layer become especially important since they will allow us to find the solution from the natural limiting condition $u = 0$ for $y = 0$.

For that, we will use what is called a "wall condition" or a simplified form which consists of disregarding the inertia term arising from the component u of velocity in the local momentum equation. Still seeking a solution for a

large Reynolds number, we shall also disregard the pressure gradient term and obtain:

$$\left(\frac{\partial \tau}{\partial y}\right)_o = \rho v_p \frac{\partial u}{\partial y} \text{ soit } \tau = \tau_p + \rho v_p u.$$

Passing to the customary variables of the wall law and expressing friction as the sum of the viscous and turbulent terms, the wall equation is written:

$$\frac{\tau}{\tau_p} = 1 + v_p^+ u^+ = \frac{\partial u^+}{\partial y^+} + F^2 k^2 y^{+2} \left(\frac{\partial u^+}{\partial y^+}\right)^2. \qquad \text{(IV.3)}$$

The turbulence term includes the corrective function which we assumed was a universal function of the ratio of turbulent friction to laminar friction (Formula II.8 and Figure 3). Since we are dealing with the vicinity of the wall, we kept $\ell = ky$ as mixing length.

IV.2.2. Results for the Physical Variable

A numerical program for the solution of Equation (IV.3) was set up and applied for a whole series of values of the transfer parameter. It allowed us to find the influence of fluid transfer on the velocity distribution in the viscous sub-layer and in the turbulent region of the wall.

Some of the profiles obtained are shown in Figure 12. We see that v_p^+ gives rise to a noticeable modification in the wall law in its usual form $u^+(y^+)$. The curves diverge markedly from that of the impermeable wall ($v_p = 0$). Moreover, Equation (IV.3) no longer gives the same logarithmic form as with an impermeable wall in a turbulent flow, but rather a solution in the form:

$$u^+ = a \log y^+ + b \log^2 y^+ + C. \qquad \text{(IV.4)}$$

We see that in the case of suction we must confine ourselves to moderate values for the rate of fluid transfer. In the case of a negative velocity

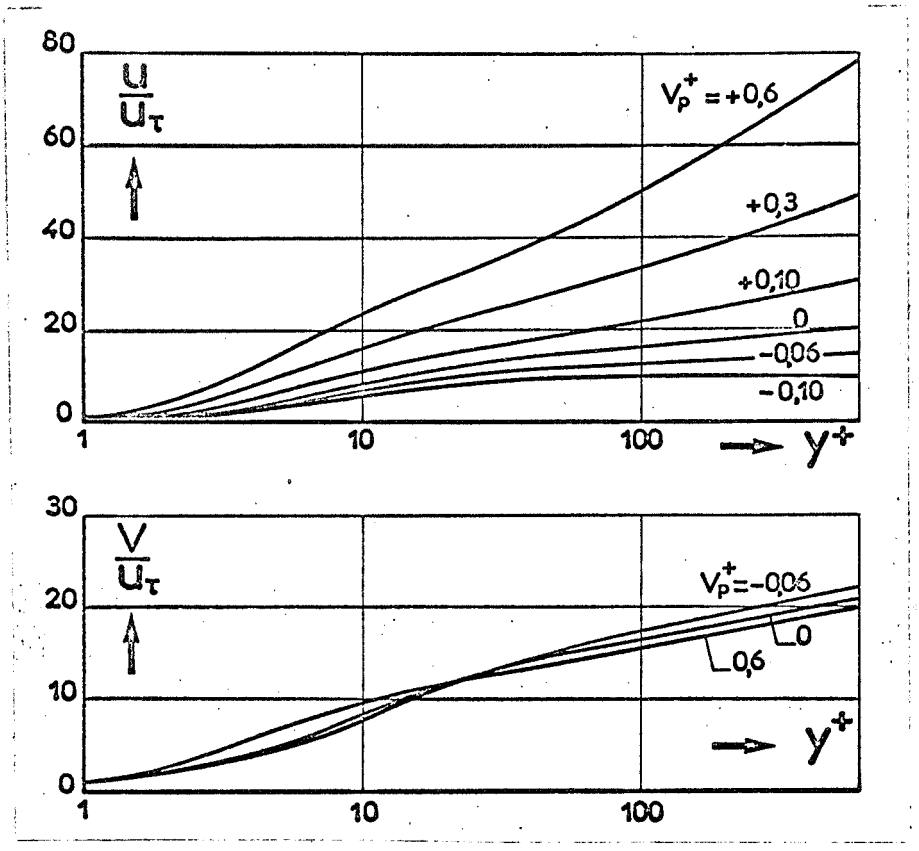

Figure 12. Wall law with fluid transfer in incompressible flow.

v_p the wall condition shows that friction τ tends toward zero when y^+ increases. We then find, as we shall explain later, that the turbulence conditions set up can no longer be attained, which obviously makes the whole technique of our research fall short of its objective.

IV.2.3. Variable Leading to a Logarithmic Law.

Confining ourselves to rates of transfer for which the turbulence conditions set up can be obtained, we must now seek a variable which will allow us to find a logarithmic law when the viscous term is negligible and the function

F^2 is equal to unity. Thus, we must transform the equation:

$$1 + v_p^+ u^+ = k^2 y^{+2} \left(\frac{\partial u^+}{\partial y^+}\right)^2 \qquad \text{(IV.5a)}$$

into an equation in the following form for the transformed variable V^+:

$$1 = k^2 y^{+2} \left(\frac{\partial V^+}{\partial y^+}\right)^2 \qquad \text{(IV.5b)}$$

We immediately find:

$$dV^+ = \frac{du^+}{(1 + v_p^+ u^+)^{1/2}} \quad \text{when} \quad V^+ = \frac{2}{v_p^+}\left\{(1 + v_p^+ u^+)^{1/2} - 1\right\} \qquad \text{(IV.6)}$$

where V^+ must vanish at the wall like u^+.

The established results for u^+ are repeated in Figure 12 for the transformed variable V^+ and we immediately see that using it allows us to rearrange the results remarkably. We once more find the logarithmic formula in the established turbulent flow: /33

$$V^+ = \frac{1}{k} \log_e y^+ + Cte.$$

The constant varies quite little with injection velocity, more especially so in the case of blowing ($v_p^+ > 0$). The numerical results let us set up the table below:

v_p^+	−0,07	−0,05	−0,03	0	0,05	0,10	0,30	0,50
C^{te}	7,1	6,1	5,7	5,25	4,9	4,7	4,3	4,2

These results confirm different attempts at analysis of experimental velocity

profiles made by Stevenson [12], in particular where it appeared that the wall law with a transformed variable was independent of the injection rate in approximated experimental dispersion up to values of v_p^+ on the order of 0.10.

IV.3. Exterior Boundary Layer - Deficient Velocity

With V^+ as the variable which gives a logarithmic form to the wall law, defined by Equation (IV.6), the variable to be used for the exterior region is $V_e^+ - V^+$.

Introducing the injection parameter P already defined:

$$P = \frac{v_p/u_e}{C_f/2} \tag{IV.7}$$

we first see that we can write the deficiency variable in the form:

$$V_e^+ - V^+ = \frac{2}{P\gamma}\left\{(1+P)^{1/2} - \left(1+P\frac{u}{u_e}\right)^{1/2}\right\} \tag{IV.8}$$

(We still use the notation $\gamma = (C_f/2)^{1/2}$). It is immediately noted that the deficiency variable is defined only for $P \geq 1$. We are still dealing with a limited application of the solution to moderate rates in the case of suction.

The technique for setting up the deficiency equation is thus identical to that which we applied to the impermeable wall:

— The independent and dependent variables are:

$$\eta = \frac{y}{\delta} \; ; \; f' = V_e^+ - V^+ = \frac{V_e - V}{u_\tau} \tag{IV.9}$$

— Friction is given by the classical formula for mixing length ($F^2 = 1$), where ℓ/δ evolves according to the assumed universal law (II.3).

— The equilibrium hypothesis is applied to the deficiency profile of the transformed variable:

$$\left(\frac{\partial f'}{\partial x}\right)_\eta = 0$$

— The hypotheses are used to express the different terms of the momentum equation taking into account the continuity equation. /34

Development leads to an ordinary differential equation written only in the shortened form:

$$\left(L^2 f''^2\right)' = -2\bar{\beta} f' - \bar{\beta}\frac{u_e}{u_e'}\frac{\gamma'}{\gamma} f' + \bar{\beta}\left(\frac{u_e}{u_e'}\frac{\delta'}{\delta} + 1\right)\eta f''$$

$$+ \frac{\bar{\beta}}{2}\frac{u_e}{u_e'}\frac{P'}{1+P} f' + \gamma\left[\cdots\right] \qquad \text{(IV.10)}$$

in which all terms multiplied by the friction coefficient γ are regrouped in the same parentheses and not expressed here.

Thus, we see the same parameters appear as in the case of an impermeable wall; the pressure gradient is still modified, however, and the injection velocity is introduced:

$$\bar{\beta} = -\frac{\delta}{\gamma(1+P)^{1/2}}\frac{u_e'}{u_e}. \qquad \text{(IV.11)}$$

There is also a parameter linked to fluid transfer: $\frac{u_e}{u_e'}\frac{P'}{1+P}$

It is again clear that an equilibrium solution requires that all these parameters be constant. We must thus first limit ourselves, as in the case of an impermeable wall, to an asymptotic solution with infinite Reynolds number $(\gamma \to 0)$.

It is also seen that an equilibrium solution will be found if P is zero; for what follows we shall use the hypothesis that

$$P = \frac{v_p/u_e}{C_f/2} = C^{te}. \qquad \text{(IV.12)}$$

To express the remaining parameters we use the technique adopted for impermeable walls, bring into play the wall friction law on the one hand and the form of the equation integrated between 0 and 1 on the other. We once more find that $\bar{\beta}\frac{u_e}{u_e'}\frac{\gamma'}{\gamma}$ tends toward zero as does γ and that the last parameter $\frac{u_e\delta'}{u_e'\delta}$ is expressed as a function of $\bar{\beta}$ as for an impermeable wall.

The deficiency differential equation with a large Reynolds number is finally:

$$\boxed{\left(L^2 f''^2\right)' = 2\bar{\beta} f' + \left(\frac{1}{f_1} + 2\bar{\beta}\right)\eta f''} \qquad \text{(IV.13a)}$$

in the case of a fluid transfer speed v_p/u_e proportional to the friction coefficient.

It brings up the only transformed pressure gradient parameter

$$\boxed{\bar{\beta} = -\frac{\delta}{\left(\frac{C_f}{2} + \frac{v_p}{u_e}\right)^{1/2}} \frac{1}{u_e}\frac{du_e}{dx}}. \qquad \text{(IV.13b)}$$

It has the same form and the same conditions at the limits as the Equation (III.9) for the impermeable case, toward which it tends when P tends toward zero.

IV.4. Law of Wall Friction /35

The relationship for the wall friction coefficient is found through the use of the overlapping of the wall law for the variable V^+ and the deficiency law found through solving Equation (IV.13) for the variable $V_e^+ - V^+$.

If (for a moderate fluid transfer) we disregard the variation of the constant in the wall law with v_p^+, for V^+ we have simply the impermeable wall law:

$$\frac{V}{u_\tau} = \frac{1}{k} \log_e \left(\frac{u_\tau y}{\nu}\right) + 5{,}25. \tag{IV.14}$$

At small values of η the deficient velocity satisfies the logarithmic relationship

$$\frac{V_e - V}{u_\tau} = -\frac{1}{k} \log_e \left(\frac{y}{\delta}\right) + D_V \tag{IV.15}$$

where D_V is the same function of $\bar{\beta}$ as in the impermeable case.

Eliminating V/u_τ from (IV.14) and (IV.15) we find (IV.16)

$$\frac{V_e}{u_\tau} = \frac{1}{k} \log_e \left(\frac{u_\tau \delta}{\nu}\right) + D_\gamma \tag{IV.16}$$

with $D_\gamma = D_V + 5{,}25$.

In view of the definition of the transformed variable (IV.6) we can write:

$$\frac{2\gamma}{v_p/u_e} \left\{ \left(1 + \frac{v_p/u_e}{\gamma^2}\right)^{1/2} - 1 \right\} = \frac{1}{k} \log_e (\gamma Re_\delta) + D_\gamma \tag{IV.17}$$

a relationship which gives the friction coefficient $\gamma = (C_f/2)^{1/2}$ as a function of the rate of transfer v_p/u_e and the Reynolds number for thickness δ; the

effects of $\bar{\beta}$ are taken into account by the constant D_γ which varies with $\bar{\beta}$ in the deficiency solution.

It is less urgent here than in the case of an impermeable wall to bring in the Reynolds number for displacement thickness. However, we find that using the simple definitions of the parameters we can give the friction law a form identical to that for the impermeable case utilizing transformed quantities for the friction coefficient and displacement thickness. Supposing then that:

$$\left(\frac{\bar{C}_f}{2}\right)^{1/2} = \frac{\gamma P}{2\left[(1+P)^{1/2}-1\right]} \; ; \; \bar{\delta}^* = \int_0^\delta \left(1 - \frac{V}{V_e}\right) dy$$

$$\bar{\mathcal{R}}_{\delta^*} = \frac{V_e \bar{\delta}^*}{\nu} = \frac{\mathcal{R}_{\delta^*}}{(1+P)^{1/2} - P_\gamma \bar{G}/4}$$

the friction law assumes the same form as Equation (III.6) for the impermeable wall, that is to say:

$$\boxed{\left(\frac{2}{\bar{C}_f}\right)^{1/2} = \frac{1}{k} \log_e\left(\bar{\mathcal{R}}_{\delta^*}\right) + D^*} \qquad \text{(IV.18)}$$

with

$$\boxed{D^* = D_\gamma - \frac{1}{k} \log_e (f_1)}$$

IV.5 Results - Comparison With Experiment

/36

IV.5.1. Velocity Profiles

Since the deficiency equation and its conditions at the limits are identical to those of an impermeable wall, the results established in Chapter III are usable in the case of a fluid transfer. Table I and the curves in Figure 5 give the profiles of transformed velocity from which those of physical velocity can be deduced. Notice again that the curves of Figure 6 give only

$L^2 f''^2$ for the transformed variable; they are linked to friction in the boundary layer by the formula:

$$L^2 f''^2 = \frac{\tau}{\tau_p + \rho v \rho \mu}.$$

The experimental results to which we may compare the solution are essentially only available for the case of a flat plate. To agree with our solution they should be regrouped along the velocity law for an impermeable flat plate when they are shown by the variable $\frac{V_e - V}{u_\tau}$. This is in fact the conclusion that different studies of mass injection led to, particularly the study by Stevenson [12].

Thus, Figure 13 shows the regrouping of Mickley and Davis's experimental data [13] by Stevenson using the transformed variable of our treatment. Our theoretical deficiency profile for a flat plate was plotted, and its agreement with experimental data is completely comparable to that already seen in the case of an impermeable wall.

Unfortunately, there are no experimental results with which we can compare the solution in the presence of pressure gradients. We must be content to note that in a physical velocity profile a velocity v_p gives rise to an effect comparable to that of positive pressure gradients, while suction gives rise to an effect comparable to that of negative pressure gradients.

IV.5.2. Wall Friction

The formulas in paragraph IV.4 (and the constants in Table II) allow us to compute the friction coefficient as a function of the Reynolds number, the wall velocity and the pressure gradient parameter. Figure 14 shows an example of a flat plate where the friction coefficient is plotted as a function of the Reynolds number for displacement thickness, the latter for different positive and negative values of the transfer rate.

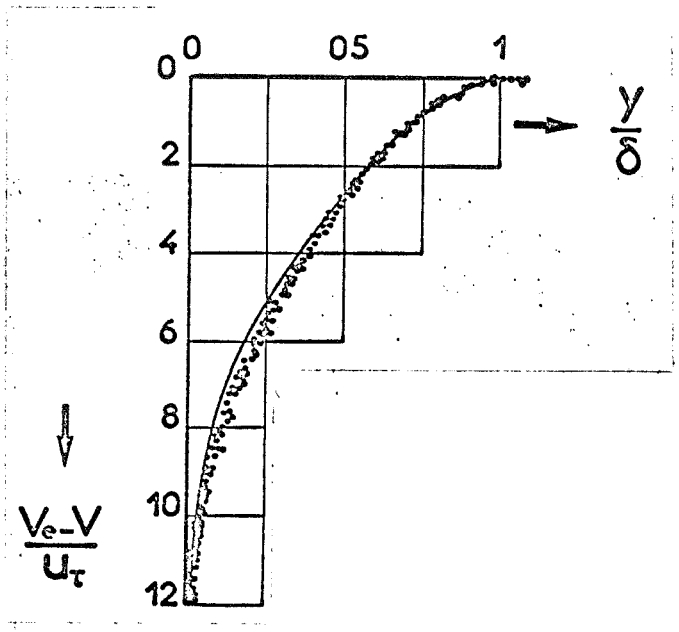

Figure 13. Law of deficient velocity with injection (Flat plate).

Also in the case of a flat plate it was possible to make a comparison between the present solution and experimental data. It is useful in showing the results to use the friction coefficient and transformed Reynolds number which lead to a formula (IV.18) identical to that for an impermeable wall. The results plotted in Figure 15 come from experimentation by Mickley and Davis [13] for blowing, and by /37
Favre, Dumas, Verollet and Coantic [14] for suction (some of the results given by these authors for higher suction rates could not be used as they exceeded the limit $P = -1$ indicated above).

We see that the experimental friction coefficients can be very reasonably regrouped with these transformed variables around the law of friction for an impermeable flat plate.

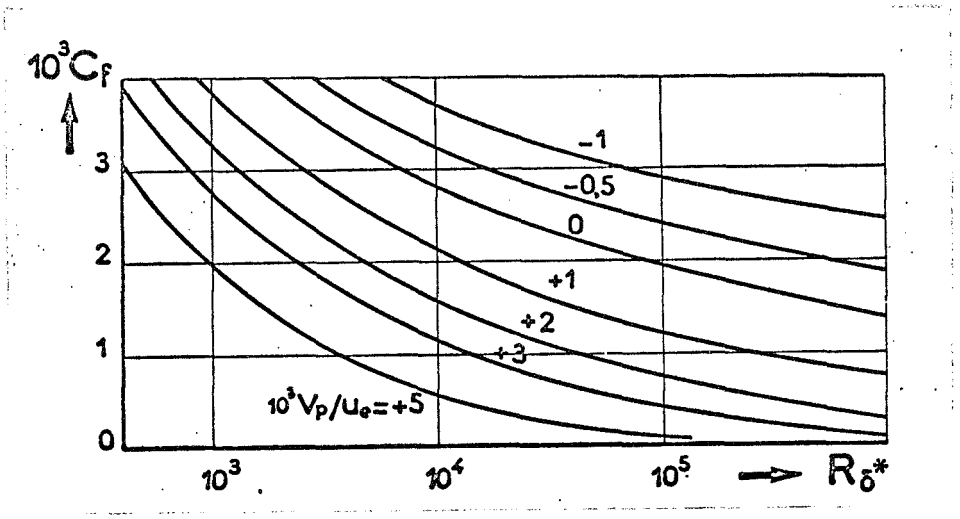

Figure 14. Wall friction coefficient with fluid transfer. (Flat plate).

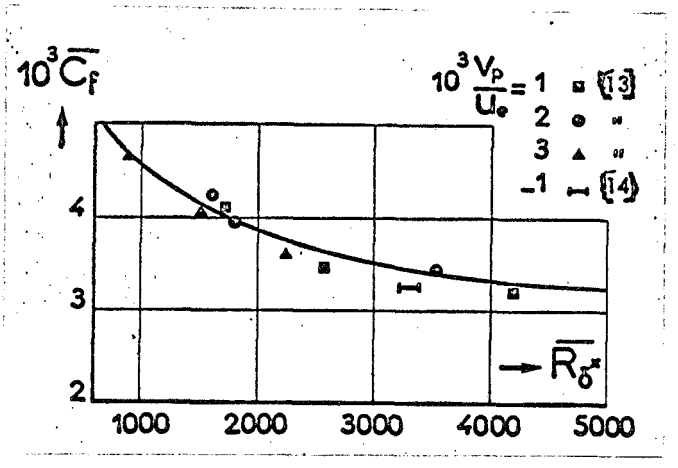

Figure 15. Wall friction coefficient with fluid transfer. Comparison with experimental results.

V. BOUNDARY LAYER IN A COMPRESSIBLE FLUID

V.1. Introduction. Preliminary Observations

The first difficulty encountered in extension to the compressible case is that the equilibrium boundary layers are no longer revealed so distinctly by experimentation.

It should be emphasized that the technique by which we propose to seek the variables which give a logarithmic form in the turbulent region of the wall is essentially the definition of the deficiency variables for which the equilibrium hypothesis will later be made in the development of the exterior equations. /38

For the velocities, we shall find that the change of variable to which we are led is the same as that which we used previously [15] in analyzing the experimental results concerning a flat sheet boundary layer. Based on the simple expression for friction by mixing length, the transformed variable for velocity [14] is introduced:

$$V=\int_0^u \left(\frac{\rho}{\rho_r}\right)^{1/2} du.$$

This variable allowed us to regroup the majority of compressible results appreciably over the wall law and deficiency law for incompressible fluids, the former up through high hypersonic Mach numbers. It should be noted here that we had to select [15] the reference at the wall in order to obtain the best return to the incompressible case. The study of the interior boundary layer through the following treatment confirms it rigorously by showing that this selection is the one which allows us to be sure that the variable in the wall law will have a universal limiting condition $(\partial V^+/\partial y^+=1$ for $y^+=0)$ and consequently to find a universal wall law.

The study will involve dealing separately with the interior and exterior regions as is now to be done for velocity and enthalpy. The overlapping of the velocity laws will lead to friction and the overlapping of the enthalpy laws will lead to heat flux at the wall.

For the interior region, the simplification made in the equations through the "wall condition" will allow us to find the results for the general case of a compressible fluid with any given Mach number.

For the exterior region, the complete equations for momentum and energy give rise to a complexity of development which has not yet allowed us to establish a solution for the general compressible case. We shall confine ourselves in the present research to presenting the solutions and the results for the case of low velocities. We should emphasize, however, that they will not be limited to fluids with constant physical properties and that they will hold for a boundary layer in which temperature may vary and cause significant heat fluxes. The simplification produced by the assumption of a low velocity is derived only from the fact that stagnant enthalpy and static enthalpy are comparable.

V.2. Interior Region - Wall Laws (General Compressible Case)

V.2.1. Wall Equations With Physical Variables

It is again obvious that the effects of fluid compressibility do not allow us to make further use of the universal law $u^+(y^+)$ and that the wall law is not established in any event for enthalpy. Those are the hypotheses concerning mixing length and the corrective function for the viscous sub-layer which will let us determine the results from the natural limiting conditions:

$$u=0 \text{ and } h=h_p \text{ when } y=0. \qquad \text{(V.1)}$$

We shall use the wall condition, that is to say, the simplified forms obtained by neglecting the inertia terms in the momentum and energy equations. Considering the case of Reynolds numbers high enough that the pressure force is also negligible, the two wall conditions are written: /39

$$\frac{\partial \tau}{\partial y} = 0 \quad \text{when} \quad \tau = \tau_p \tag{V.2}$$

$$\frac{\partial (u\tau - \phi)}{\partial y} = 0 \qquad \phi = u\tau_p + \phi_p. \tag{V.3}$$

The wall equation for velocities is found by writing τ as the sum of the viscous and turbulent terms:

$$\tau = \tau_p = \mu \frac{\partial u}{\partial y} + F^2 \rho k^2 y^2 \left(\frac{\partial u}{\partial y}\right)^2; \tag{V.4}$$

The turbulent term includes the corrective function F^2 which depends on τ_t / τ_l because of the universal relationship assumed in the scheme. Since we are dealing with the neighborhood of the wall, we again grant that $l = ky$.

The wall equation for enthalpies is found by writing ϕ as the sum of the laminar and turbulent terms. Bringing apparent turbulent viscosity and conductivity and the turbulent Prandtl number $\mathcal{P}_t = \varepsilon C_p / \chi$ into the latter term, we have:

$$\phi_t = -\frac{\chi}{C_p} \frac{\partial h}{\partial y}$$

$$\tau_t = \varepsilon \frac{\partial u}{\partial y}$$

whence $$-\phi_t = \frac{\tau_t}{\mathcal{P}_t} \frac{\partial h / \partial y}{\partial u / \partial y};$$

and consequently the wall equation is written:

$$-\phi = -(u\tau_p + \phi_p) = \frac{\lambda}{C_p}\frac{\partial h}{\partial y} + \frac{F^2 \rho k^2 y^2}{P_t}\frac{\partial h}{\partial y}\frac{\partial u}{\partial y}. \qquad \text{(V.5)}$$

In what follows we shall assume that the turbulent Prandtl number is constant. The two wall Equations (V.4) and (V.5) are clearly coupled and should be solved simultaneously. We should note in particular that F^2 depends on $\frac{\tau_t}{\tau_\ell} = \frac{\rho \ell^2}{\mu}\frac{\partial u}{\partial y}$ where ρ and μ are variable and dependent on enthalpy.

V.2.2. Transformed Variables Leading to Logarithmic Laws.

We must now seek the transformed variables which give the wall laws for velocity and enthalpy a logarithmic form when the viscous term is negligible and the function F^2 is equal to unity.

Velocities. The friction velocity u_τ and the distance variable y^+ are formed with the wall conditions:

$$u_\tau = \left(\frac{\tau_p}{\rho_p}\right)^{1/2}, \quad y^+ = \frac{\rho_p u_\tau y}{\mu_p},$$

so the change of variable which allows us to find the desired result is the one used in [15]: /140

$$V = \int_0^u \left(\frac{\rho}{\rho_p}\right)^{1/2} du. \qquad \text{(V.6)}$$

It allows us to write the wall Equation (V.4) in the form:

$$\frac{\mu}{\mu_p}\left(\frac{\rho_p}{\rho}\right)^{1/2}\frac{\partial V^+}{\partial y^+} + F^{-2}k^2 y^{+2}\left(\frac{\partial V^+}{\partial y^+}\right)^2 = 1, \qquad \text{(V.7)}$$

which, when the viscous term is negligible, gives the expected result when $F^2 = 1$:

$$\frac{\partial V^+}{\partial y^+} = \frac{1}{k y^+} \quad \text{whence} \quad V^+ = \frac{1}{k} \log_e y^+ + \text{constant}$$

Enthalpies. In the established turbulent case, the wall equation for enthalpies becomes:

$$-(u\tau_p + \phi_p) = \rho \frac{k^2 y^2}{\mathcal{P}_t} \frac{\partial h}{\partial y} \frac{\partial u}{\partial y},$$

an equation which the desired change of variables should reduce to a form with a logarithmic solution, i.e.:

$$k y^+ \frac{\partial H^+}{\partial y^+} = 1 \quad \text{whence} \quad H^+ = \frac{1}{k} \log_e y^+ + \text{constant} \qquad \text{(V.8)}$$

(taking into account the result already obtained for velocity).

To arrive at it, we first replace static enthalpy with a kind of turbulent stagnant enthalpy:

$$h_{it} = h + \mathcal{P}_t \frac{u^2}{2}. \qquad \text{(V.9)}$$

We apply the same change of compressibility variable to it as to velocity:

$$H = \int_0^{h_{it}} \left(\frac{\rho}{\rho_p}\right)^{1/2} d h_{it}. \qquad \text{(V.10)}$$

It is next related to a "friction enthalpy" H_τ to define the wall variable H^+ which gives the desired logarithmic form:

$$H^+ = \frac{H}{\mathcal{P}_t H_\tau} \quad \text{with} \quad H_\tau = -\frac{\phi_p u_\tau}{\tau_p}. \qquad \text{(V.11)}$$

The complete wall Equation (V.5) is finally written:

$$\left(\frac{\mu}{\mu_p}\right)\left(\frac{\rho_p}{\rho}\right)^{1/2}\left[\frac{\mathcal{P}_t}{\mathcal{P}}\frac{\partial H^+}{\partial y^+}+\left(\frac{\mathcal{P}_t}{\mathcal{P}}-1\right)\frac{u_t\tau_p}{\phi_p}u^+\frac{\partial V^+}{\partial y^+}\right]+F^2k^2y^{+2}\frac{\partial H^+}{\partial y^+}\frac{\partial V^+}{\partial y^+}=1. \qquad (V.12)$$

It is this equation which should be solved together with (V.7) to determine the wall laws for enthalpy and velocity. $\mathcal{P}_t$ and $\mathcal{P}$ are respectively the turbulent Prandtl number and the Prandtl number $\mu c_p/\lambda$.

V.2.3. Results for the Wall Laws.

If Equations (V.7) and (V.12) lead to the common classical logarithmic form in the established turbulent case, the influence of μ and ρ, which occurs with the viscous terms in integration from the wall, is liable a priori to give rise to a constant which varies with the given data (h_p, M_e, $\mathcal{P}_t$) of the case which may be considered. However, we may hope that the variation of the constant will remain small, since the variables V^+ and H^+ are subject to well-determined limiting conditions: /41

— when $y^+=0$: $\quad V^+=H^+=0;\ \frac{\partial V^+}{\partial y^+}=1;\ \frac{\partial H^+}{\partial y^+}=\frac{\mathcal{P}}{\mathcal{P}_t}$

— for large y^+ : $\quad \frac{\partial V^+}{\partial y^+}=\frac{\partial H^+}{\partial y^+}=\frac{1}{ky^+}$.

This is what we wanted to verify by establishing a program of simultaneous numerical solution of Equations (V.7) and (V.12) and applying it to different cases of compressibility from subsonic to hypersonic.

Two examples of results obtained shown in Figures 16a and 16b correspond to two extreme cases. The first ($M_e=0{,}1$; $T_p/T_f=0{,}9$) is close to the conditions with constant physical properties of the "incompressible" solution. The second ($M_e=10$; $T_p/T_f=0{,}3$) corresponds to current test conditions in a hypersonic

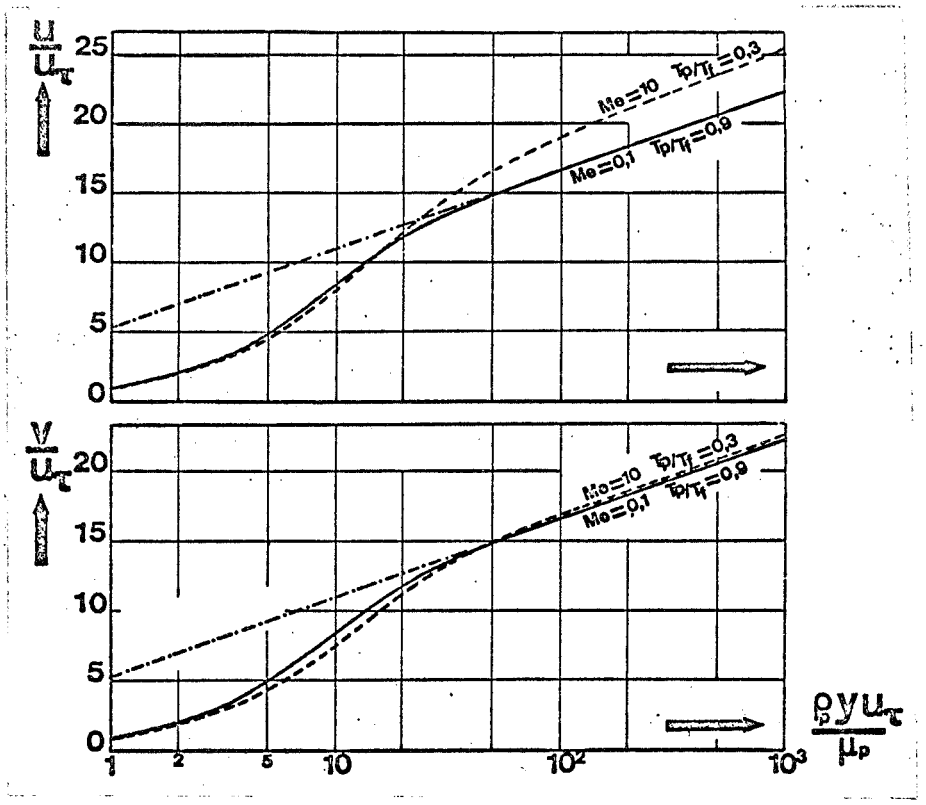

Figure 16a. Wall law in compressible fluid: velocities.

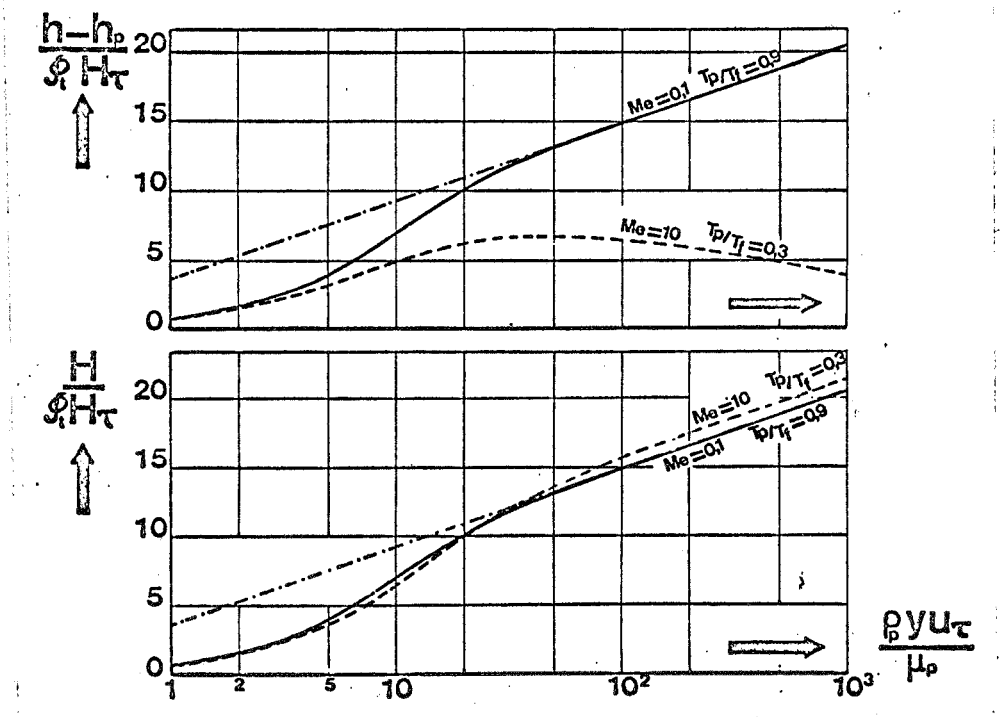

Figure 16b. Wall law in compressible fluid: enthalpies.

wind tunnel. Results for transformed and physical variables are shown together.

We see right away that the wall laws for physical quantities u and h are clearly affected by compressibility. The influence is particularly marked in the case of enthalpies: at $M_e = 10$ h passes through a maximum, as it should physically in a case where exterior enthalpy is less than the wall enthalpy.

The use of transformed variables changes the results conspicuously. The wall law for velocities is only slightly modified in the viscous sub-layer. The wall law for enthalpies produces a logarithmic portion the constant of which is influenced little by compressibility.

Overlooking these small deviations, we grant in the following that the turbulent wall laws for velocity and enthalpy are given by the universal relationships: /42

$$\boxed{\frac{V}{u_\tau} = \frac{1}{k} \log_e \left(\frac{\rho_p u_\tau y}{\mu_p} \right) + 5{,}25} \qquad \text{(V.13)}$$

$$\boxed{\frac{H}{\mathcal{P}_t H_\tau} = \frac{1}{k} \log_e \left(\frac{\rho_p u_\tau y}{\mu_p} \right) + 3{,}60} \qquad \text{(V.14)}$$

V.3. Exterior Regions - Deficiency Laws (Case of Small Velocities: $M_e \to 0$)

The complexity of the development to which the complete energy and momentum equations lead in compressible fluids has so far limited the treatment of the exterior region in the case of a low velocity. The simplification is brought about by the fact that the stagnant enthalpies are comparable to static enthalpies. For the enthalpy variable we thus have: $h_i = h_{it} = h$.

We should note that the transformed variable is then linked directly to physical enthalpy:

$$H=\int_{h_p}^{h}\left(\frac{\rho}{\rho_p}\right)^{1/2}dh=2h_p^{1/2}\left(h^{1/2}-h_p^{1/2}\right) \qquad \text{(V.15a)}$$

if we assume that the gas is calorifically perfect.

Let us also recall the definition of transformed velocity: /43

$$V=\int_0^u\left(\frac{\rho}{\rho_p}\right)^{1/2}du. \qquad \text{(V.15b)}$$

The technique to be used in establishing the deficiency equations is still the same, but it now involves the equations for momentum and energy.

— The independent and dependent variables are:

$$\boxed{\eta=\frac{y}{\delta}}\ ;\ \boxed{f'=\frac{V_e-V}{u_\tau}}\ ;\ \boxed{g'=\frac{H_e-H}{\mathcal{P}_t\,H_\tau}} \qquad \text{(V.16)}$$

— The equilibrium hypothesis is applied for the two transformed variables

$$\left(\frac{\partial f'}{\partial x}\right)_\eta=0 \quad \text{and} \quad \left(\frac{\partial g'}{\partial x}\right)_\eta=0.$$

— Friction and heat transfer are expressed by the classical mixing length formula, and the latter evolves according to the universal relationship (II.3):

$$\tau=\rho\ell^2\left(\frac{\partial u}{\partial y}\right)^2;\ \phi=-\rho\frac{\ell^2}{\mathcal{P}_t}\frac{\partial h}{\partial y}\frac{\partial u}{\partial y}.$$

— The hypotheses are introduced into the local equations for momentum and energy, which are written respectively:

$$\rho u \frac{\partial u}{\partial x} + \rho v \frac{\partial u}{\partial y} = \rho_e u_e \frac{du_e}{dx} + \frac{\partial}{\partial y}\left(\rho l^2 \left(\frac{\partial u}{\partial y}\right)^2\right)$$

$$\rho u \frac{\partial h}{\partial x} + \rho v \frac{\partial h}{\partial y} = \frac{\partial}{\partial y}\left(\rho \frac{l^2}{\mathcal{P}_t} \frac{\partial h}{\partial y} \frac{\partial u}{\partial y}\right).$$

To these are joined the continuity equation, and we hypothesize a perfect gas with constant specific heats, due to which enthalpy is inversely proportional to density.

Once more simplifying through the notation:

$$\bar{\gamma} = \frac{u_\tau}{V_e} \; ; \; \sigma = \frac{H_\tau}{H_e} \qquad \text{(V.17)}$$

we shall here confine ourselves to a discussion of the order of magnitude of the parameters, without writing out the developments which occur as factors of the derivatives of f and g in the two equations. These parameters are:

$$\bar{\gamma}, \sigma, \frac{\bar{\gamma}'}{\bar{\gamma}} \frac{V_e}{V_e'}, \frac{\sigma'}{\sigma} \frac{V_e}{V_e'}, \frac{\bar{\gamma}^2 V_e^2}{\sigma H_e}, \frac{H_e'}{H_e} \frac{V_e}{V_e'}, \frac{V_e}{V_e'} \frac{\delta'}{\delta}, \frac{V_e}{V_e'} \frac{\rho_P'}{\rho_P}, \frac{\delta}{\bar{\gamma}} \frac{V_e'}{V_e}.$$

— Taking the case of an infinite Reynolds number, γ and σ tend toward zero. The form of the relationships for friction and wall heat flux shows, on the other hand, that $\frac{\bar{\gamma}'}{\bar{\gamma}} \frac{V_e}{V_e'}$ and $\frac{\sigma'}{\sigma} \frac{V_e}{V_e'}$ are on the order of γ; the same is true for $\frac{\bar{\gamma}^2 V_e^2}{\sigma H_e}$.

— $\frac{H_e'}{H_e} \frac{V_e}{V_e'}$ is on the order of M_e^2 and thus negligible at low velocities. /44

— Finally, we can express the parameters $\frac{V_e \delta'}{V_e' \delta}$ and $\frac{V_e \rho_P'}{V_e' \rho_P}$ by requiring the two equations integrated from 0 to 1 to satisfy limiting conditions, particularly at $\tau/\tau_P = \phi/\phi_P = 1$ for $\eta = 0$. With momentum and energy we find respectively:

$$-\bar{\beta}\left\{\frac{V_e}{V_e'}\left(\frac{\delta'}{\delta}+\frac{\rho_p'}{\rho_p}\right)\right\}=\frac{1}{f_1}+3\bar{\beta}$$

$$-\bar{\beta}\left\{\frac{V_e}{V_e'}\left(\frac{\delta'}{\delta}+\frac{\rho_p'}{\rho_p}\right)\right\}=\frac{1}{\mathcal{P}_t g_1}+\bar{\beta} \quad \text{whence} \quad \frac{1}{\mathcal{P}_t g_1}=\frac{1}{f_1}+2\bar{\beta}. \tag{V.18}$$

— The only remaining parameter is that of the pressure gradient, which it is interesting to introduce in the transformed form:

$$\boxed{\bar{\beta}=-\frac{\delta}{\bar{\delta}}\frac{V_e'}{V_e}\left(\frac{h_p}{h_e}\right)^{1/2}} \tag{V.19}$$

With this form we find that the momentum equation leads to a differential equation which is the same as the one established for the incompressible case:

$$\boxed{\left(L^2 f''^2\right)'=\left(2\bar{\beta}+\frac{1}{f_1}\right)\eta f''+2\bar{\beta}f} \tag{V.20}$$

The energy equation leads to the differential equation:

$$\boxed{\left(L^2 f'' g'\right)'=\frac{\eta g''}{g_1}} \tag{V.21}$$

The corresponding limiting conditions are:

$$\eta=0 : f_0=g_0=0$$
$$\eta=1 : f_1'=g_1'=g_1''=0.$$

V.4. Friction and Heat Transfer at the Wall

The relationships for heat transfer and wall friction are found through the use of the overlapping wall laws, given in their turbulent portions by the solution of Equations (V.20) and (V.21). The form of the equations and their solutions show that transformed deficient velocity and enthalpy are given at

low values of η by the logarithmic equations:

$$\frac{V_e - V}{u_\tau} = -\frac{1}{k} \log_e \frac{y}{\delta} + D_V \qquad \text{(V.22)}$$

$$\frac{H_e - H}{\mathcal{P}_t H_\tau} = -\frac{1}{k} \log_e \frac{y}{\delta} + D_H \qquad \text{(V.23)}$$

where D_V is the same function of $\bar{\beta}$ as in the incompressible case, since the equation is the same, and where D_H is a function of $\bar{\beta}$ which results in the solution of (V.21). /145

Eliminating V/u_τ and $H/\mathcal{P}_t H_\tau$ from (V.13) and (V.22) on the one hand and from (V.14) and (V.23) on the other hand, we find:

$$\frac{V_e}{u_\tau} = \frac{1}{k} \log_e \frac{\rho_p u_\tau \delta}{\mu_p} + D_\gamma \quad \text{with} \quad D_\gamma = D_V + 5{,}25$$

$$\frac{H_e}{\mathcal{P}_t H_\tau} = \frac{1}{k} \log_e \frac{\rho_p u_\tau \delta}{\mu_p} + D_\sigma \quad \text{with} \quad D_\sigma = D_H + 3{,}60 .$$

We then introduce transformed coefficients and Reynolds number:

$$\frac{\bar{C}_f}{2} = \frac{\tau_p}{\rho_p V_e^2} ; \quad \bar{C}h = \frac{\phi_p}{\rho_p V_e H_e} ; \quad \overline{\mathcal{R}e}_\delta = \frac{\rho_p V_e \delta}{\mu_p} , \qquad \text{(V.24)}$$

in order to write the preceding equations in the form of relationships for the friction coefficient and the heat transfer coefficient:

$$\boxed{\left(\frac{2}{\bar{C}_f}\right)^{1/2} = \frac{1}{k} \log_e \left(\overline{\mathcal{R}e}_\delta \left(\frac{\bar{C}_f}{2}\right)^{1/2}\right) + D_\gamma} \qquad \text{(V.25)}$$

$$\boxed{\frac{(\bar{C}_f/2)^{1/2}}{\mathcal{P}_t \bar{C}_h} = \frac{1}{k} \log_e \left(\overline{\mathcal{R}e}_\delta \left(\frac{\bar{C}_f}{2}\right)^{1/2}\right) + D_\sigma} . \qquad \text{(V.26)}$$

We note that the friction law in this form is the same as that we found in the incompressible case. The same is true when using transformed displacement thickness and Reynolds number:

$$\overline{\delta^*} = \int_0^{\delta} \left(1 - \frac{V}{V_e}\right) dy \; ; \quad \overline{\mathcal{R}_{\delta^*}} = \frac{\rho_p V_e \overline{\delta^*}}{\mu_p} ,$$

and the friction law is then written:

$$\boxed{\left(\frac{2}{\overline{C_f}}\right)^{1/2} = \frac{1}{k} \log_e \overline{\mathcal{R}_{\delta^*}} + D^*} \quad \text{with} \quad D^* = D_\gamma - \frac{1}{k} \log_e f_1 . \tag{V.27}$$

Finally, we define the analogy factor $\bar{s}$ as the ratio of the transformed coefficients and express it by the formula:

$$\boxed{\frac{1}{\bar{s}} = \frac{C_f}{2\overline{C_h}} = \mathcal{P}_t \left\{1 + D_s \left(\frac{\overline{C_f}}{2}\right)^{1/2}\right\}} \tag{V.28}$$

with

$$D_s = D_\sigma - D_\gamma .$$

The variation of D_s with $\bar{\beta}$ will show the influence of pressure gradients on the analogy factor.

V.5. Presentation of Results

/146

Since the deficiency Equation (V.20) for velocities is identical to that for the incompressible case, the results of Chapter III are directly applicable. Table I and Figure 5 give the profiles for transformed deficient velocity for different values of the transformed parameter $\bar{\beta}$. The friction distributions in Figure 6 are likewise applicable to the compressible case.

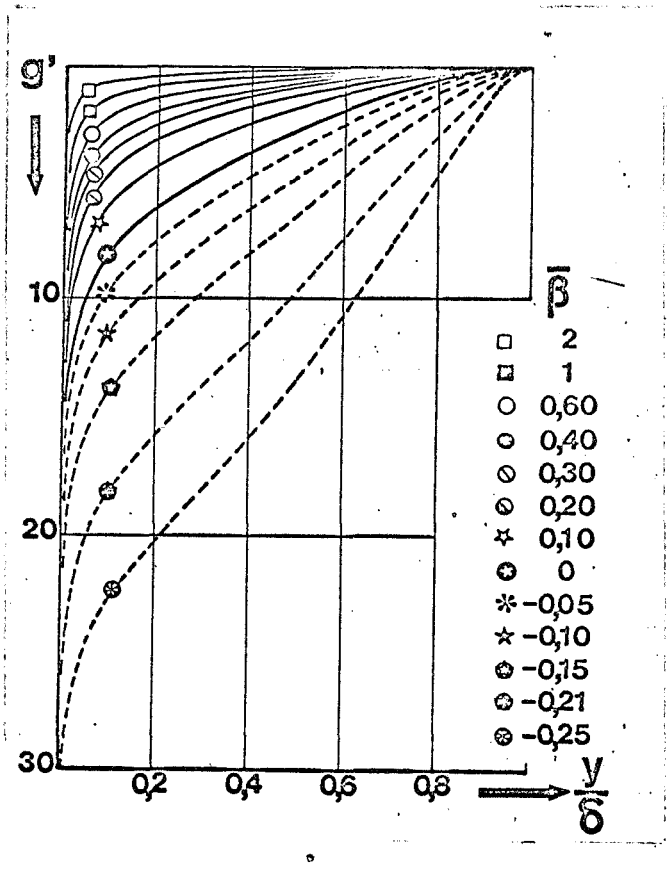

Figure 17a. Deficient enthalpies.

$$g' = \frac{H_e - H}{\mathcal{P}_t H_\tau}$$

The profiles for the enthalpy variable g' were also found by solving Equation (V.21) by a numerical program comparable to that used for velocities. The numerical values of the transformed deficient enthalpy are also shown in Table I. The profiles are plotted in Figures 17a and 17b. By using a logarithmic scale for η, we find that the curves are linear for low values of η with a slope of 1/k.

Heat flux $\frac{\phi}{\phi_p} = L^2 f'' g''$ distributions are shown in Figure 18 for different values of the pressure gradient parameter. It should be pointed out that a singularity occurs with reference to enthalpy at the lower limiting value $\bar{\beta} = -0{,}44$ mentioned in Chapter III. For this limit, we have:

$$\frac{1}{\mathcal{P}_t g_1} = \frac{1}{f_1} + 2\bar{\beta} = 0 \quad , \text{when } g_1 \to \infty$$

The solution for Equation (V.21) is $g' = \infty$ in the entire boundary layer except when $\eta = 1$ where $g' = 0$. From that, it should be concluded that H_τ is zero. We emphasize that transformed enthalpy H, however, is not infinite but zero over the entire boundary layer (h = constant = h_p) except when $\eta = 1$ where it rejoins H_e.

It is interesting to analyze the preceding results by examining the evolution curves of enthalpy as function of velocity. Some such curves are given in Figure 19 for the more easily interpreted physical values, H/H_e and V/V_e, which are linked to f' and g' by the relationships:

147

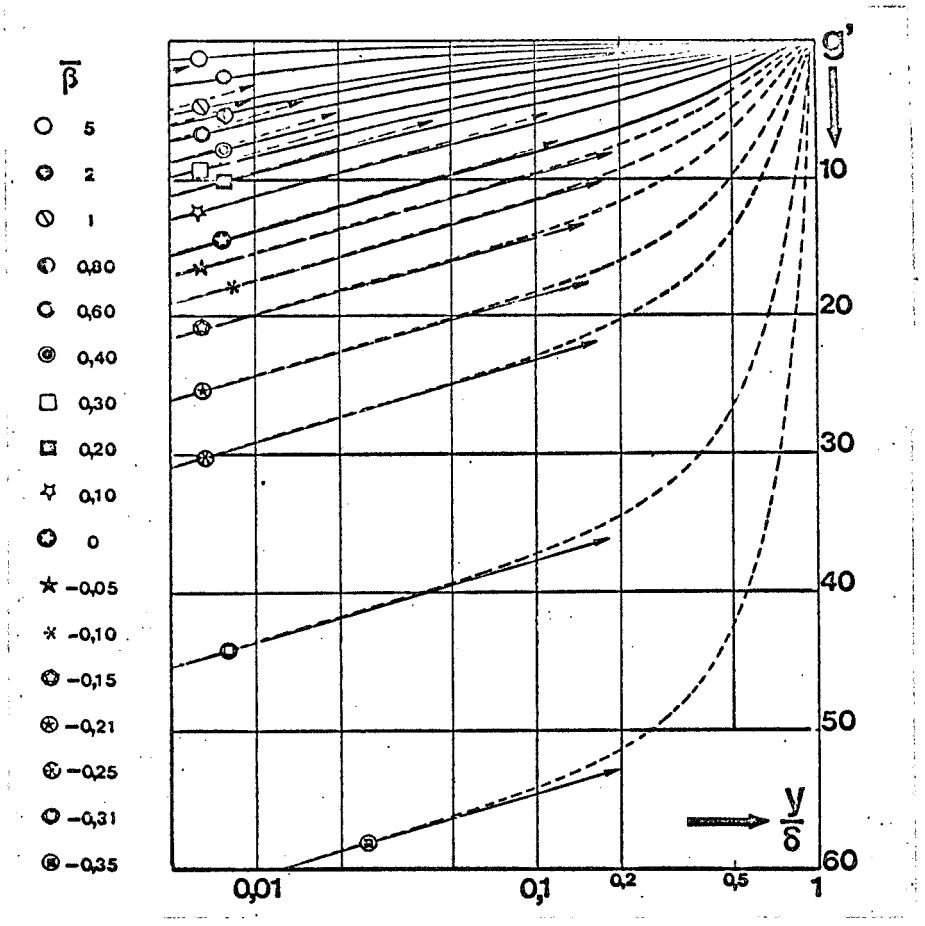

Figure 17b. Deficient enthalpies (logarithmic scale for y/δ).

148

$$\frac{H}{H_e} = 1 - \sigma \mathcal{P}_t g' \qquad \frac{V}{V_e} = 1 - \bar{\gamma} f'.$$

Thus, they depend through γ and σ on the Reynolds number. For the example presented, we chose a high value ($\mathcal{R}_\delta = 50\,000$).

In the case of a flat plate ($\bar{\beta} = 0$) the relationship is linear. The figure

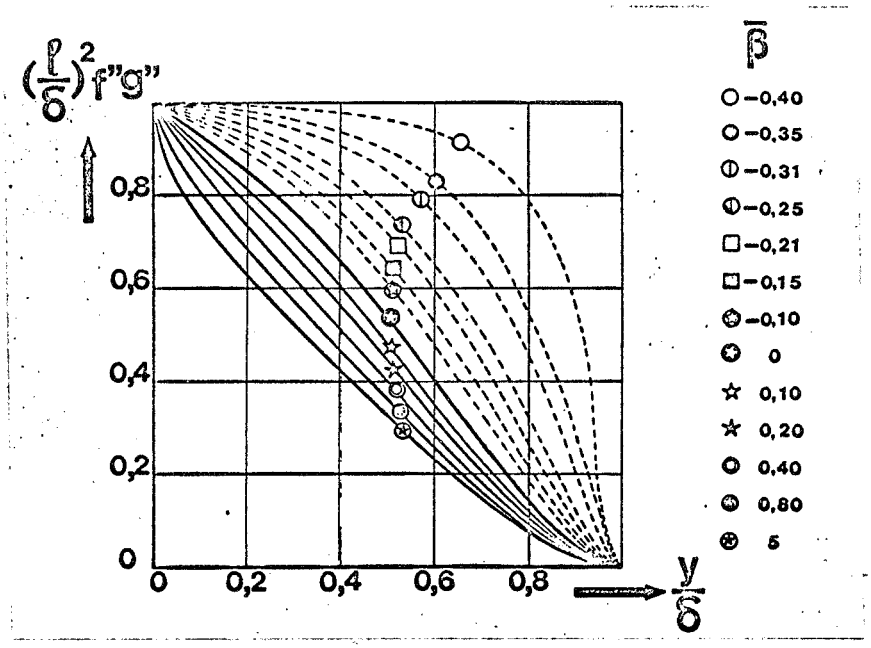

Figure 18. Distributions of heat flux ϕ/ϕ_p.

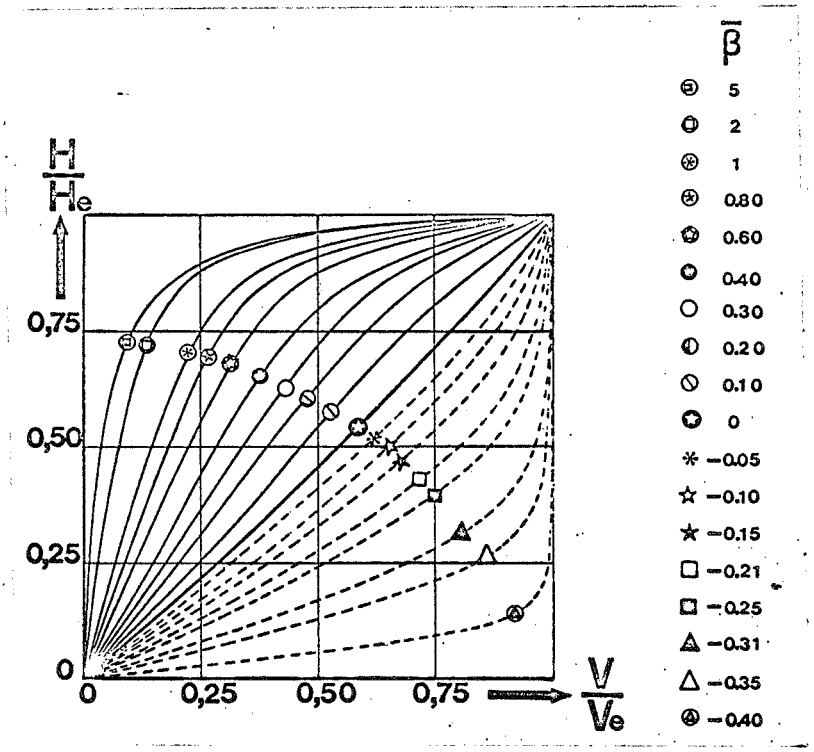

Figure 19. Enthalpy-velocity profiles. $\overline{R_\delta} = 50\,000$.

shows that the pressure gradients have a considerable influence on the enthalpy-velocity relationship.

We can see that $\bar{\beta}$ is the product of $(h_p/h_e)^{1/2}$ and a term more especially characteristic of the pressure gradient. Decreasing h_p makes the absolute value of $\bar{\beta}$ decrease and brings the curves closer to that of the flat plate: the effect of the pressure gradients is less, the colder the wall is. These results are likened to those for a laminar boundary layer set up in particular by similar solutions by Cohen and Reshotko [16].

Finally, Figure 20 shows the variation in the analogy factor $\bar{\lambda}$ with $\bar{\beta}$ for different values of the Reynolds number. Formula (V.28) shows that $\bar{\lambda}$ depends on the Reynolds number through $\bar{C}_f^{1/2}$ and thus varies slowly with $\bar{R}_\delta$. It depends on the pressure gradient through the constant D_λ, and on the other hand varies considerably with $\bar{\beta}$.

For a flat plate D_λ is quite small in order that the analogy factor will not differ much from $\bar{\lambda} = 1/\phi_t^*$. The negative pressure gradients cause a decrease in the analogy factor, $\bar{\lambda}$ becoming zero at the lower limit $\bar{\beta} = -0{,}44$. The positive pressure gradients cause an increase in $\bar{\lambda}$ which becomes infinite at separation, where friction is zero when heat flux is not. It is likewise clear, in view of the definition of $\bar{\beta}$, that the effect of the pressure gradients on the analogy factor is less, the colder the wall.

VI. FINAL OBSERVATIONS AND CONCLUSIONS

/49

The criticism that can be made of the proposed treatment is that the separation into exterior and interior regions assumes that the established turbulent conditions are in fact attained when the overlapping of the wall law and the deficiency law comes into play. In fact, we can find important cases where this condition is not satisfied and where the principle of separation into two regions is not applicable. It is interesting to dwell on this point as the hypothesis for the viscous sublayer corrective function allows us to make some interesting observations on what might be the behavior in such cases of turbulent friction.

In Paragraph II.1.3 we saw that the ratio of turbulent friction to laminar friction can be related to total friction and mixing length through the formula:

$$2\frac{\tau_t}{\tau_l} = -1 + \sqrt{1 + 4Y\left\{1 - \exp\left(\frac{-Y^{1/2}}{26k}\right)\right\}^2}, \text{ with } Y = \frac{\rho \tau l^2}{\mu^2}.$$

The formula shows that τ_t / τ_e is zero at the wall ($l = 0$) as is normal, but it is important to note that τ_t / τ_e can also become zero at a distance from the wall if total friction itself tends toward zero.

This is what was found when calculating the interior region with strong suction when the wall condition was $\tau = \tau_p + \rho v_p u$ with a negative v_p, causing total friction to decrease and tend toward zero. Figure 21 shows the results obtained for τ_t / τ_e by solving the wall Equation (IV.3) for different values of the fluid transfer rate. We see that for moderate blowing or suction, τ_t / τ_e reaches quite high values, so that the established turbulent conditions may be regarded as actually attained. At velocities v_p^+ lower than -0.07, on the other hand, turbulent friction reaches only much lower values. In the case of strong suction, we are faced with a veritable laminarization of the entire interior region.

/50

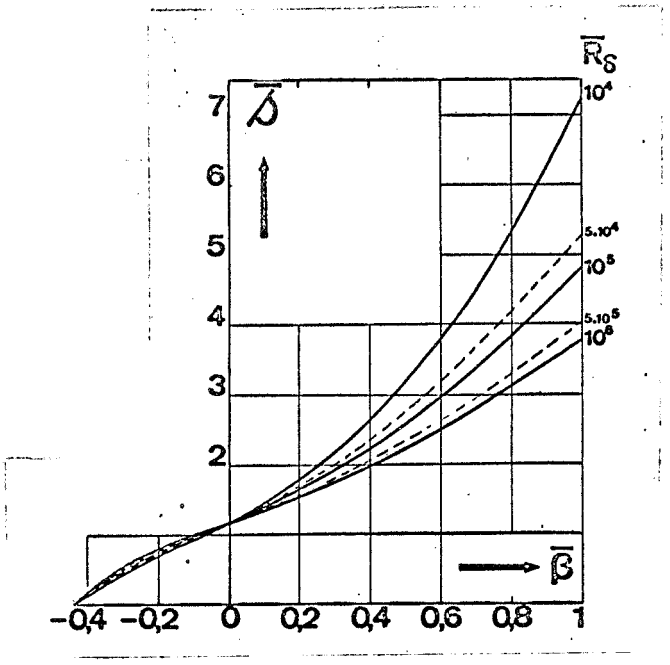

Figure 20. Analogy factor as a function of $\overline{\beta}$.

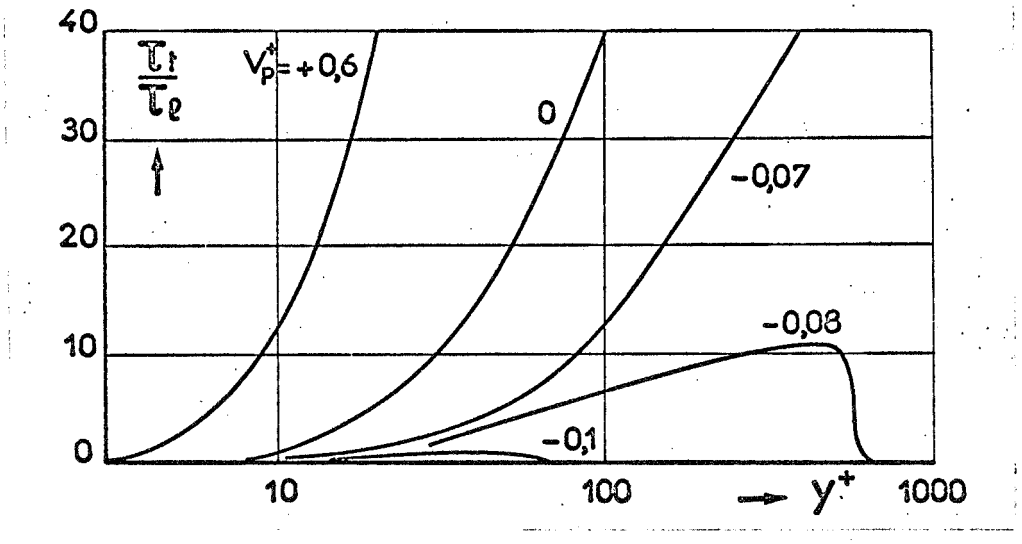

Figure 21. Wall law with fluid transfer. Turbulent friction in the interior region.

Because it is linked to the rapid decrease in total friction, the phenomenon should likewise be produced by strong negative pressure gradients, if the Reynolds number is not too high.

Aside from these special cases, for which the proposed scheme appears in need of further clarification, we can conclude that the improved hypotheses of the mixing length concept have allowed us to end up with some coherent results for a whole range of turbulent boundary layer problems.

Their application to equilibrium boundary layers was interesting in that it showed in a systematic manner the effects of the principal factors which may come into play in the problems.

We should emphasize that it allowed us to find results hitherto not available on boundary layers with fluid transfer at the wall in the presence of pressure gradients.

In a compressible fluid, much work still remains to be done to give results for the general case for any Mach number. It is unlikely, however, that the conclusions will be fundamentally different from those shown by the present research at low speeds.

We should, henceforth, insist on the fact that the effects of pressure gradients are at least as important in the thermal boundary layer as in the dynamic boundary layer.

The results established for the enthalpy-velocity relationship and the analogy factor are altogether comparable to those of similar solutions for laminar boundary layers.

Manuscript submitted November 21, 1969.

$\frac{y}{\delta}$ \ β	−0.442		−0.40		−0.35		−0.31		−0.25		−0.21	
	f'	g'	f'	g'	f'	g'	f'	g'	f'	g'	f'	g'
0.0	∞	∞	∞	∞	∞	∞	∞	∞	∞	∞	∞	∞
0.0010	13.529		13.80	152.66	14.18	66.03	14.47	49.12	15.07	34.61	15.49	29.86
0.0022	11.735		12.00	150.83	12.38	64.21	12.67	47.30	13.27	32.78	13.69	28.04
0.0035	10.638		10.91	149.69	11.28	63.08	11.57	46.17	12.16	31.66	12.58	26.92
0.0049	9.828		10.09	148.85	10.47	62.23	10.75	45.32	11.35	30.82	11.76	26.08
0.0064	9.173		9.44	148.15	9.81	61.54	10.09	44.63	10.69	30.13	11.10	25.39
0.0082	8.617	∞	8.88	147.56	9.25	60.94	9.53	44.04	10.12	29.54	10.54	24.80
0.0100	8.129		8.39	147.02	8.76	60.41	9.04	43.51	9.63	29.01	10.04	24.28
0.0121	7.690		7.95	146.54	8.32	59.93	8.59	43.03	9.18	28.54	9.59	23.81
0.0145	7.289		7.55	146.09	7.91	59.48	8.19	42.58	8.77	28.09	9.18	23.37
0.0170	6.918		7.17	145.66	7.54	59.06	7.81	42.16	8.39	27.68	8.80	22.95
0.0198	6.572		6.83	145.26	7.19	58.66	7.46	41.76	8.03	27.28	8.44	22.56
0.0230	6.245	∞	6.50	144.87	6.86	58.27	7.13	41.38	7.70	26.91	8.10	22.19
0.0264	5.935		6.18	144.49	6.54	57.90	6.81	41.01	7.38	26.54	7.77	21.83
0.0302	5.640		5.89	144.13	6.24	57.54	6.51	40.65	7.07	26.19	7.46	21.48
0.0344	5.357		5.60	143.77	5.95	57.18	6.22	40.30	6.77	25.84	7.17	21.13
0.0391	5.085		5.33	143.41	5.68	56.83	5.94	39.95	6.49	25.50	6.88	20.80
0.0442	4.824		5.06	143.06	5.41	56.49	5.67	39.61	6.21	25.17	6.60	20.47
0.0499	4.571	∞	4.81	142.71	5.15	56.14	5.40	39.27	5.95	24.83	6.33	20.14
0.0561	4.326		4.56	142.36	4.90	55.80	5.15	38.93	5.69	24.50	6.07	19.82
0.0630	4.089		4.32	142.01	4.65	55.45	4.90	38.59	5.43	24.17	5.81	19.49
0.0707	3.859		4.09	141.65	4.41	55.11	4.66	38.25	5.19	23.84	5.56	19.17
0.0791	3.635		3.86	141.29	4.18	54.75	4.42	37.90	4.94	23.51	5.31	18.84
0.0884	3.417		3.64	140.92	3.95	54.40	4.19	37.55	4.70	23.17	5.07	18.51
0.0987	3.204	∞	3.42	140.55	3.73	54.03	3.97	37.19	4.47	22.83	4.83	18.18
0.1101	2.996		3.21	140.16	3.51	53.65	3.74	36.82	4.24	22.48	4.59	17.84
0.1227	2.792		3.00	139.75	3.30	53.26	3.53	36.44	4.01	22.12	4.35	17.49
0.1366	2.593		2.80	139.33	3.09	52.86	3.31	36.05	3.79	21.74	4.12	17.13
0.1519	2.398		2.60	138.88	2.88	52.43	3.10	35.63	3.56	21.35	3.89	16.76
0.1668	2.206		2.40	138.41	2.68	51.97	2.89	35.20	3.34	20.95	3.66	16.37
0.1875	2.018	∞	2.20	137.89	2.47	51.49	2.68	34.73	3.12	20.52	3.43	15.96
0.2082	1.832		2.01	137.34	2.27	50.97	2.47	34.23	2.89	20.06	3.20	15.53
0.2310	1.650		1.82	136.73	2.07	50.39	2.26	33.68	2.67	19.56	2.96	15.06
0.2562	1.470		1.63	136.04	1.87	49.76	2.05	33.08	2.45	19.02	2.73	14.56
0.2841	1.294		1.45	135.27	1.67	49.05	1.85	32.42	2.22	18.43	2.49	14.02
0.3149	1.122		1.27	134.38	1.48	48.24	1.64	31.66	1.99	17.78	2.25	13.42
0.3488	0.954	∞	1.09	133.35	1.28	47.31	1.44	30.80	1.77	17.04	2.00	12.76
0.3864	0.792		0.91	132.11	1.09	46.22	1.23	29.81	1.54	16.21	1.75	12.01
0.4279	0.638		0.75	130.60	0.91	44.92	1.03	28.63	1.31	15.26	1.51	11.18
0.4737	0.494		0.59	128.71	0.73	43.34	0.84	27.24	1.08	14.15	1.26	10.23
0.5243	0.363		0.44	126.29	0.56	41.37	0.66	25.54	0.86	12.87	1.02	9.15
0.5802	0.248		0.31	123.07	0.41	38.87	0.49	23.44	0.66	11.37	0.78	7.92
0.6419	0.153	∞	0.20	118.58	0.28	35.60	0.33	20.81	0.46	9.60	0.56	6.52
0.7101	0.081		0.11	111.93	0.16	31.19	0.20	17.45	0.29	7.53	0.36	4.96
0.7854	0.033		0.05	101.12	0.08	25.00	0.10	13.10	0.16	5.17	0.19	3.27
0.8687	0.007		0.01	80.81	0.03	15.99	0.03	7.54	0.06	2.60	0.07	1.56
0.9606	0.000	∞	0.00	31.26	0.00	3.51	0.00	1.36	0.00	0.38	0.01	0.21
1.0000	0.0	0.0	0.0	0.0	0.0	0.0	0.0	0.0	0.0	0.0	0.0	0.0

Table 1a. Velocity and deficient enthalpies.

$\bar{y}/\bar{\delta}_1$ \ $\bar{\beta}$ →	−0.15		−0.10		−0.05		0.0		0.10		0.20	
	f'	g'	f'	g'	f'	g'	f'	g'	f'	g'	f'	g'
0.0	∞	∞	∞	∞	∞	∞	∞	∞	∞	∞	∞	∞
0.0010	16.17	25.41	16.81	22.83	17.59	20.75	18.48	19.11	20.58	16.67	23.12	14.91
0.0022	14.36	23.59	15.01	21.01	15.78	18.93	16.67	17.30	18.76	14.87	21.29	13.11
0.0035	13.26	22.47	13.90	19.89	14.67	17.82	15.55	16.18	17.64	13.76	20.17	12.02
0.0049	12.43	21.63	13.08	19.05	13.85	16.99	14.73	15.35	16.81	12.94	19.32	11.20
0.0064	11.77	20.95	12.41	18.37	13.18	16.31	14.05	14.68	16.13	12.27	18.64	10.55
0.0082	11.20	20.36	11.84	17.79	12.60	15.73	13.48	14.10	15.55	11.70	18.05	9.99
0.0100	10.70	19.84	11.33	17.27	12.10	15.22	12.97	13.59	15.03	11.20	17.52	9.50
0.0121	10.25	19.37	10.88	16.81	11.64	14.75	12.51	13.13	14.56	10.75	17.04	9.06
0.0145	9.83	18.93	10.46	16.37	11.22	14.32	12.08	12.71	14.13	10.34	16.60	8.65
0.0170	9.45	18.53	10.07	15.97	10.83	13.92	11.69	12.31	13.72	9.95	16.18	8.26
0.0198	9.09	18.14	9.71	15.59	10.46	13.54	11.31	11.94	13.34	9.59	15.79	7.93
0.0230	8.74	17.77	9.36	15.22	10.11	13.18	10.96	11.58	12.98	9.25	15.41	7.60
0.0264	8.42	17.41	9.03	14.87	9.77	12.84	10.62	11.24	12.63	8.92	15.04	7.29
0.0302	8.10	17.07	8.72	14.53	9.45	12.50	10.29	10.92	12.29	8.60	14.69	7.00
0.0344	7.80	16.73	8.41	14.20	9.14	12.18	9.98	10.60	11.96	8.30	14.34	6.71
0.0391	7.51	16.40	8.11	13.88	8.84	11.86	9.67	10.29	11.64	8.01	14.00	6.44
0.0442	7.23	16.08	7.82	13.56	8.55	11.55	9.37	9.99	11.32	7.73	13.66	6.17
0.0499	6.95	15.76	7.54	13.25	8.26	11.25	9.08	9.70	11.01	7.45	13.33	5.92
0.0561	6.68	15.45	7.27	12.94	7.98	10.95	8.79	9.41	10.70	7.18	13.00	5.67
0.0630	6.42	15.13	7.00	12.63	7.70	10.65	8.50	9.12	10.40	6.92	12.67	5.43
0.0707	6.16	14.82	6.73	12.33	7.43	10.36	8.22	8.84	10.10	6.66	12.35	5.20
0.0791	5.90	14.50	6.47	12.03	7.16	10.07	7.94	8.56	9.80	6.41	12.02	4.97
0.0884	5.65	14.19	6.21	11.72	6.89	9.78	7.67	8.28	9.50	6.15	11.68	4.75
0.0987	5.40	13.87	5.96	11.41	6.63	9.48	7.39	8.00	9.19	5.91	11.35	4.53
0.1101	5.16	13.54	5.70	11.10	6.36	9.19	7.11	7.72	8.89	5.66	11.00	4.32
0.1227	4.91	13.21	5.45	10.79	6.10	8.89	6.84	7.44	8.58	5.42	10.66	4.11
0.1366	4.67	12.88	5.20	10.47	5.83	8.59	6.56	7.16	8.27	5.17	10.30	3.90
0.1519	4.43	12.53	4.94	10.14	5.57	8.28	6.28	6.87	7.95	4.93	9.93	3.69
0.1688	4.18	12.16	4.69	9.80	5.30	7.97	5.99	6.58	7.62	4.68	9.55	3.49
0.1875	3.94	11.79	4.43	9.45	5.02	7.64	5.70	6.28	7.28	4.43	9.16	3.28
0.2082	3.69	11.39	4.17	9.08	4.74	7.31	5.40	5.98	6.93	4.18	8.74	3.08
0.2310	3.44	10.97	3.90	8.69	4.46	6.95	5.09	5.66	6.56	3.93	8.31	2.87
0.2562	3.19	10.52	3.63	8.29	4.16	6.59	4.77	5.33	6.16	3.67	7.85	2.66
0.2841	2.93	10.04	3.35	7.85	3.86	6.20	4.43	4.99	5.78	3.40	7.37	2.45
0.3149	2.66	9.51	3.06	7.38	3.54	5.79	4.08	4.63	5.36	3.12	6.85	2.24
0.3488	2.39	8.94	2.76	6.88	3.21	5.35	3.72	4.25	4.91	2.84	6.29	2.02
0.3864	2.11	8.31	2.46	6.34	2.87	4.89	3.34	3.85	4.43	2.54	5.70	1.80
0.4279	1.83	7.62	2.14	5.75	2.52	4.39	2.94	3.43	3.93	2.24	5.07	1.57
0.4737	1.55	6.85	1.82	5.11	2.15	3.86	2.53	2.99	3.40	1.93	4.40	1.35
0.5243	1.26	6.01	1.50	4.42	1.78	3.30	2.10	2.53	2.84	1.61	3.70	1.12
0.5802	0.98	5.08	1.18	3.68	1.41	2.71	1.67	2.06	2.27	1.29	2.97	0.89
0.6419	0.72	4.07	0.86	2.89	1.04	2.10	1.24	1.58	1.70	0.97	2.24	0.66
0.7101	0.47	2.99	0.57	2.08	0.70	1.49	0.84	1.10	1.15	0.67	1.52	0.45
0.7854	0.26	1.89	0.32	1.28	0.39	0.90	0.47	0.66	0.65	0.39	0.86	0.26
0.8687	0.10	0.86	0.12	0.57	0.15	0.39	0.18	0.28	0.25	0.17	0.34	0.11
0.9606	0.01	0.11	0.01	0.07	0.01	0.05	0.02	0.03	0.02	0.02	0.03	0.01
1.0000	0.0	0.0	0.0	0.0	0.0	0.0	0.0	0.0	0.0	0.0	0.0	0.0

Table 1b. Velocity and deficient enthalpies.

y/δ \ $\bar{\beta}$	0.30		0.40		0.50		0.60		0.69		0.80	
	f'	g'	f'	g'	f'	g'	f'	g'	f'	g'	f'	g'
0.0	∞	∞	∞	∞	∞	∞	∞	∞	∞	∞	∞	∞
0.0010	25.98	13.59	29.25	12.49	32.65	11.62	36.32	10.86	39.91	10.25	43.93	9.66
0.0022	24.14	11.80	27.41	10.72	30.80	9.86	34.45	9.11	38.02	8.51	42.03	7.94
0.0035	23.01	10.71	26.26	9.64	29.64	8.79	33.27	8.07	36.83	7.48	40.82	6.93
0.0049	22.16	9.91	25.40	8.85	28.76	8.01	32.38	7.30	35.92	6.73	39.88	6.20
0.0064	21.46	9.26	24.69	8.22	28.03	7.40	31.64	6.70	35.16	6.15	39.10	5.63
0.0082	20.86	8.72	24.07	7.68	27.40	6.88	30.98	6.20	34.49	5.66	38.40	5.16
0.0100	20.32	8.24	23.52	7.22	26.83	6.43	30.40	5.76	33.88	5.24	37.77	4.76
0.0121	19.83	7.81	23.01	6.80	26.31	6.03	29.85	5.38	33.31	4.88	37.17	4.42
0.0145	19.37	7.42	22.54	6.43	25.81	5.67	29.33	5.04	32.77	4.55	36.60	4.11
0.0170	18.94	7.06	22.09	6.09	25.34	5.35	28.84	4.74	32.25	4.26	36.05	3.83
0.0198	18.53	6.73	21.66	5.77	24.89	5.05	28.36	4.45	31.74	4.00	35.52	3.59
0.0230	18.13	6.42	21.24	5.48	24.45	4.77	27.89	4.19	31.25	3.75	34.99	3.36
0.0264	17.75	6.12	20.83	5.20	24.02	4.51	27.43	3.95	30.75	3.53	34.46	3.15
0.0302	17.37	5.84	20.43	4.94	23.59	4.27	26.97	3.73	30.27	3.32	33.93	2.96
0.0344	17.01	5.58	20.04	4.70	23.17	4.04	26.52	3.52	29.78	3.13	33.41	2.78
0.0391	16.64	5.32	19.65	4.46	22.75	3.83	26.06	3.33	29.28	2.95	32.87	2.62
0.0442	16.28	5.08	19.26	4.24	22.33	3.63	25.60	3.14	28.79	2.78	32.33	2.46
0.0499	15.93	4.85	18.87	4.03	21.90	3.44	25.14	2.97	28.28	2.62	31.78	2.32
0.0561	15.57	4.62	18.48	3.83	21.47	3.25	24.67	2.80	27.77	2.47	31.22	2.18
0.0630	15.21	4.40	18.08	3.63	21.03	3.08	24.18	2.65	27.24	2.33	30.64	2.05
0.0707	14.85	4.20	17.68	3.45	20.59	2.91	23.69	2.50	26.70	2.20	30.05	1.93
0.0791	14.48	3.99	17.28	3.27	20.14	2.76	23.19	2.36	26.15	2.07	29.44	1.82
0.0884	14.11	3.80	16.86	3.10	19.67	2.60	22.67	2.22	25.58	1.95	28.81	1.71
0.0987	13.74	3.61	16.43	2.93	19.20	2.46	22.14	2.10	24.99	1.83	28.15	1.61
0.1101	13.35	3.42	16.00	2.77	18.70	2.32	21.59	1.97	24.37	1.72	27.47	1.51
0.1227	12.95	3.24	15.55	2.62	18.19	2.18	21.01	1.86	23.73	1.62	26.76	1.42
0.1366	12.55	3.06	15.08	2.46	17.66	2.05	20.41	1.74	23.07	1.52	26.01	1.33
0.1519	12.12	2.89	14.59	2.32	17.11	1.93	19.78	1.63	22.36	1.42	25.23	1.24
0.1688	11.68	2.72	14.08	2.17	16.52	1.80	19.12	1.52	21.62	1.33	24.40	1.16
0.1875	11.22	2.55	13.54	2.03	15.91	1.68	18.41	1.42	20.84	1.23	23.52	1.08
0.2082	10.74	2.38	12.98	1.89	15.25	1.56	17.67	1.32	20.00	1.14	22.58	1.00
0.2310	10.23	2.21	12.37	1.75	14.56	1.45	16.87	1.22	19.10	1.06	21.58	0.92
0.2562	9.68	2.04	11.73	1.61	13.81	1.33	16.02	1.12	18.14	0.97	20.50	0.84
0.2841	9.10	1.87	11.04	1.48	13.01	1.21	15.09	1.02	17.10	0.88	19.33	0.77
0.3149	8.48	1.70	10.30	1.34	12.14	1.10	14.10	0.92	15.98	0.80	18.07	0.69
0.3488	7.81	1.53	9.50	1.20	11.21	0.98	13.02	0.82	14.76	0.71	16.69	0.62
0.3864	7.09	1.36	8.63	1.06	10.20	0.87	11.85	0.73	13.44	0.63	15.21	0.55
0.4279	6.32	1.18	7.71	0.92	9.11	0.75	10.59	0.63	12.02	0.54	13.60	0.47
0.4737	5.50	1.01	6.71	0.78	7.94	0.64	9.24	0.53	10.49	0.46	11.87	0.40
0.5243	4.63	0.83	5.66	0.64	6.70	0.52	7.80	0.44	8.85	0.38	10.02	0.33
0.5802	3.73	0.66	4.56	0.51	5.40	0.41	6.29	0.34	7.15	0.30	8.09	0.26
0.6419	2.81	0.49	3.44	0.38	4.08	0.31	4.75	0.25	5.40	0.22	6.12	0.19
0.7101	1.91	0.33	2.34	0.26	2.78	0.21	3.24	0.17	3.69	0.15	4.17	0.13
0.7854	1.09	0.19	1.34	0.15	1.59	0.12	1.85	0.10	2.11	0.09	2.39	0.07
0.8687	0.43	0.08	0.52	0.06	0.62	0.05	0.73	0.04	0.83	0.03	0.94	0.03
0.9606	0.04	0.01	0.05	0.01	0.06	0.01	0.07	0.00	0.08	0.00	0.09	0.00
1.0000	0.0	0.0	0.0	0.0	0.0	0.0	0.0	0.0	0.0	0.0	0.0	0.0

Table 1c. Velocity and deficient enthalpies .

$\frac{y}{\delta_t}$ \ $\bar{\beta}$ →	0.90		1.00		1.50		2.00		2.42		2.99	
	f'	g'	f'	g'	f'	g'	f'	g'	f'	g'	f'	g'
0.0	∞	∞	∞	∞	∞	∞	∞	∞	∞	∞	∞	∞
0.0010	47.93	9.15	51.93	8.71	72.72	7.01	94.37	5.84	113.02	5.10	138.17	4.35
0.0022	46.01	7.46	49.98	7.03	70.63	5.45	92.09	4.41	110.56	3.78	135.44	3.16
0.0035	44.77	6.46	48.73	6.06	69.22	4.57	90.51	3.64	108.81	3.08	133.43	2.55
0.0049	43.82	5.75	47.74	5.37	68.10	3.98	89.20	3.12	107.33	2.63	131.72	2.16
0.0064	43.01	5.20	46.91	4.83	67.11	3.53	88.04	2.74	106.00	2.30	130.15	1.89
0.0062	42.29	4.75	46.16	4.40	66.21	3.17	86.95	2.45	104.75	2.05	128.67	1.67
0.0100	41.63	4.37	45.47	4.03	65.36	2.88	85.92	2.21	103.54	1.84	127.23	1.50
0.0121	41.00	4.04	44.82	3.72	64.54	2.63	84.91	2.01	102.36	1.67	125.81	1.36
0.0145	40.40	3.75	44.19	3.44	63.73	2.42	83.91	1.84	101.19	1.53	124.40	1.24
0.0170	39.82	3.49	43.58	3.20	62.94	2.23	82.92	1.69	100.02	1.40	122.99	1.14
0.0198	39.25	3.25	42.98	2.98	62.15	2.06	81.92	1.56	98.84	1.29	121.56	1.05
0.0230	38.69	3.04	42.38	2.78	61.36	1.92	80.91	1.45	97.65	1.20	120.11	0.97
0.0264	38.13	2.85	41.78	2.60	60.55	1.78	79.89	1.35	96.43	1.11	118.63	0.90
0.0302	37.56	2.67	41.17	2.43	59.74	1.66	78.85	1.25	95.19	1.03	117.12	0.84
0.0344	36.99	2.50	40.56	2.28	58.91	1.55	77.78	1.17	93.92	0.96	115.57	0.78
0.0391	36.42	2.35	39.94	2.14	58.06	1.45	76.69	1.09	92.61	0.90	113.97	0.73
0.0442	35.83	2.21	39.31	2.01	57.19	1.36	75.56	1.02	91.26	0.84	112.33	0.68
0.0499	35.23	2.08	38.67	1.88	56.29	1.27	74.40	0.95	89.87	0.78	110.62	0.63
0.0561	34.62	1.95	38.01	1.77	55.37	1.19	73.20	0.89	88.43	0.73	108.86	0.59
0.0630	33.99	1.84	37.33	1.66	54.41	1.12	71.95	0.84	86.94	0.69	107.03	0.55
0.0707	33.35	1.73	36.63	1.56	53.43	1.05	70.66	0.78	85.39	0.64	105.13	0.52
0.0791	32.68	1.63	35.90	1.47	52.40	0.98	69.32	0.73	83.77	0.60	103.15	0.49
0.0884	31.99	1.53	35.15	1.38	51.33	0.92	67.92	0.69	82.09	0.56	101.08	0.46
0.0987	31.27	1.44	34.37	1.30	50.21	0.86	66.46	0.64	80.33	0.53	98.92	0.43
0.1101	30.52	1.35	33.55	1.22	49.04	0.81	64.92	0.60	78.48	0.49	96.65	0.40
0.1227	29.74	1.26	32.70	1.14	47.82	0.76	63.31	0.56	76.54	0.46	94.27	0.37
0.1366	28.92	1.18	31.80	1.07	46.53	0.71	61.61	0.53	74.49	0.43	91.75	0.35
0.1519	28.05	1.10	30.85	1.00	45.16	0.66	59.82	0.49	72.32	0.40	89.08	0.32
0.1688	27.14	1.03	29.85	0.93	43.71	0.62	57.91	0.46	70.02	0.38	86.25	0.30
0.1875	26.16	0.96	28.78	0.86	42.17	0.57	55.87	0.42	67.56	0.35	83.23	0.28
0.2082	25.12	0.89	27.65	0.80	40.52	0.53	53.69	0.39	64.93	0.32	79.99	0.26
0.2310	24.01	0.82	26.42	0.74	38.74	0.49	51.35	0.36	62.10	0.30	76.50	0.24
0.2562	22.81	0.75	25.11	0.67	36.83	0.45	48.82	0.33	59.04	0.27	72.74	0.22
0.2841	21.52	0.68	23.69	0.61	34.76	0.41	46.07	0.30	55.73	0.25	68.66	0.20
0.3149	20.11	0.62	22.15	0.55	32.51	0.37	43.10	0.27	52.13	0.22	64.23	0.18
0.3488	18.59	0.55	20.47	0.49	30.06	0.33	39.86	0.24	48.21	0.20	59.41	0.16
0.3864	16.94	0.48	18.65	0.43	27.40	0.29	36.33	0.21	43.95	0.17	54.16	0.14
0.4279	15.15	0.42	16.68	0.38	24.51	0.25	32.51	0.18	39.33	0.15	48.47	0.12
0.4737	13.22	0.35	14.56	0.32	21.41	0.21	28.40	0.15	34.35	0.13	42.34	0.10
0.5243	11.17	0.29	12.30	0.26	18.09	0.17	24.00	0.13	29.04	0.10	35.79	0.08
0.5802	9.02	0.23	9.94	0.20	14.61	0.13	19.39	0.10	23.46	0.08	28.91	0.07
0.6419	6.82	0.17	7.51	0.15	11.05	0.10	14.67	0.07	17.75	0.06	21.87	0.05
0.7101	4.65	0.11	5.13	0.10	7.55	0.07	10.02	0.05	12.12	0.04	14.94	0.03
0.7854	2.66	0.07	2.93	0.06	4.32	0.04	5.73	0.03	6.94	0.02	8.55	0.02
0.8687	1.04	0.03	1.15	0.02	1.70	0.02	2.25	0.01	2.72	0.01	3.36	0.01
0.9606	0.10	0.00	0.11	0.00	0.16	0.00	0.21	0.00	0.26	0.00	0.32	0.00
1.0000	0.0	0.0	0.0	0.0	0.0	0.0	0.0	0.0	0.0	0.0	0.0	0.0

Table 1d. Velocity and deficient enthalpies.

$\bar{\beta}\rightarrow$ / $\frac{y}{\delta}\downarrow$	4.00		5.00		6.00		6.99		7.99		10.00	
	f'	g'	f'	g'	f'	g'	f'	g'	f'	g'	f'	g'
0.0	∞	∞	∞	∞	∞	∞	∞	∞	∞	∞	∞	∞
0.0010	182.78	3.44	227.63	2.83	272.54	2.39	317.17	2.08	362.00	1.83	452.79	1.47
0.0022	179.52	2.44	223.80	1.98	268.10	1.66	312.12	1.43	356.32	1.26	445.82	1.01
0.0035	177.04	1.95	220.81	1.57	264.60	1.32	308.10	1.13	351.77	0.99	440.18	0.80
0.0049	174.87	1.64	218.18	1.32	261.49	1.11	304.51	0.95	347.69	0.83	435.12	0.67
0.0064	172.87	1.43	215.73	1.15	258.59	0.96	301.15	0.82	343.88	0.72	430.37	0.57
0.0082	170.96	1.26	213.38	1.01	255.80	0.84	297.92	0.72	340.20	0.63	425.78	0.51
0.0100	169.10	1.13	211.09	0.91	253.07	0.75	294.75	0.65	336.59	0.57	421.28	0.45
0.0121	167.26	1.02	208.81	0.82	250.36	0.68	291.60	0.58	333.00	0.51	416.81	0.41
0.0145	165.42	0.93	206.54	0.75	247.64	0.62	288.45	0.53	329.41	0.47	412.32	0.37
0.0170	163.57	0.85	204.24	0.68	244.90	0.57	285.27	0.49	325.78	0.43	407.76	0.34
0.0198	161.69	0.79	201.92	0.63	242.12	0.52	282.04	0.45	322.10	0.39	403.18	0.31
0.0230	159.79	0.73	199.55	0.58	239.29	0.48	278.75	0.41	318.35	0.36	398.49	0.29
0.0264	157.84	0.67	197.13	0.54	236.40	0.45	275.38	0.38	314.51	0.33	393.69	0.27
0.0302	155.85	0.62	194.65	0.50	233.43	0.41	271.93	0.36	310.57	0.31	388.77	0.25
0.0344	153.80	0.58	192.10	0.46	230.38	0.39	268.38	0.33	306.52	0.29	383.70	0.23
0.0391	151.69	0.54	189.47	0.43	227.24	0.36	264.72	0.31	302.34	0.27	378.47	0.21
0.0442	149.51	0.51	186.76	0.40	223.99	0.34	260.94	0.29	298.02	0.25	373.07	0.20
0.0499	147.26	0.47	183.95	0.38	220.62	0.31	257.02	0.27	293.55	0.23	367.48	0.19
0.0561	144.92	0.44	181.04	0.35	217.14	0.29	252.96	0.25	288.92	0.22	361.68	0.18
0.0630	142.50	0.41	178.02	0.33	213.51	0.27	248.75	0.23	284.10	0.21	355.66	0.16
0.0707	139.97	0.39	174.87	0.31	209.75	0.26	244.36	0.22	279.09	0.19	349.39	0.15
0.0791	137.35	0.36	171.60	0.29	205.82	0.24	239.78	0.21	273.87	0.18	342.85	0.14
0.0884	134.60	0.34	168.17	0.27	201.71	0.23	235.00	0.19	268.41	0.17	336.03	0.13
0.0987	131.73	0.32	164.59	0.25	197.42	0.21	230.00	0.18	262.70	0.16	328.87	0.13
0.1101	128.71	0.30	160.82	0.24	192.91	0.20	224.75	0.17	256.70	0.15	321.37	0.12
0.1227	125.54	0.28	156.87	0.22	188.16	0.18	219.22	0.16	250.39	0.14	313.46	0.11
0.1366	122.20	0.26	152.69	0.21	183.15	0.17	213.38	0.15	243.72	0.13	305.12	0.10
0.1519	118.65	0.24	148.26	0.19	177.84	0.16	207.20	0.14	236.66	0.12	296.28	0.10
0.1688	114.88	0.23	143.55	0.18	172.20	0.15	200.62	0.13	229.15	0.11	286.88	0.09
0.1875	110.86	0.21	138.53	0.17	166.17	0.14	193.61	0.12	221.14	0.10	276.85	0.08
0.2082	106.55	0.19	133.15	0.15	159.72	0.13	186.09	0.11	212.55	0.10	266.10	0.08
0.2310	101.91	0.18	127.35	0.14	152.77	0.12	178.00	0.10	203.31	0.09	254.53	0.07
0.2562	96.90	0.16	121.10	0.13	145.26	0.11	169.25	0.09	193.32	0.08	242.03	0.06
0.2841	91.47	0.15	114.31	0.12	137.13	0.10	159.77	0.08	182.50	0.07	228.48	0.06
0.3149	85.57	0.13	106.94	0.11	128.28	0.09	149.47	0.08	170.73	0.07	213.74	0.05
0.3488	79.15	0.12	98.91	0.09	118.66	0.08	138.25	0.07	157.92	0.06	197.71	0.05
0.3864	72.16	0.10	90.18	0.08	108.19	0.07	126.05	0.06	143.98	0.05	180.26	0.04
0.4279	64.58	0.09	80.71	0.07	96.83	0.06	112.82	0.05	128.86	0.04	161.34	0.04
0.4737	56.41	0.08	70.50	0.06	84.57	0.05	98.54	0.04	112.56	0.04	140.92	0.03
0.5243	47.69	0.06	59.60	0.05	71.50	0.04	83.31	0.04	95.16	0.03	119.14	0.02
0.5802	38.53	0.05	48.15	0.04	57.77	0.03	67.31	0.03	76.88	0.02	96.26	0.02
0.6419	29.15	0.04	36.43	0.03	43.71	0.02	50.93	0.02	58.17	0.02	72.83	0.01
0.7101	19.91	0.02	24.89	0.02	29.86	0.02	34.79	0.01	39.74	0.01	49.76	0.01
0.7854	11.40	0.01	14.25	0.01	17.09	0.01	19.92	0.01	22.75	0.01	28.48	0.01
0.8687	4.47	0.01	5.59	0.00	6.71	0.00	7.82	0.00	8.93	0.00	11.18	0.00
0.9606	0.42	0.00	0.53	0.00	0.64	0.00	0.74	0.00	0.85	0.00	1.06	0.00
1.0000	0.0	0.0	0.0	0.0	0.0	0.0	0.0	0.0	0.0	0.0	0.0	0.0

Table 1e. Velocity and deficient enthalpies.

$\bar{\beta}$	D_γ	D_σ	f_1	g_1	G	P	T
-0.442	2.03	∞	1.13	∞	3.77	0.	0.16
-0.40	2.30	139.51	1.23	115.29	3.84	0.01	0.17
-0.35	2.69	52.89	1.38	37.72	3.97	0.03	0.19
-0.31	2.97	35.98	1.49	23.88	4.07	0.04	0.20
-0.25	3.57	21.47	1.73	12.95	4.32	0.09	0.23
-0.21	4.00	16.72	1.90	9.72	4.51	0.12	0.26
-0.15	4.67	12.26	2.18	6.91	4.85	0.16	0.30
-0.10	5.32	9.68	2.45	5.43	5.19	0.22	0.35
-0.05	6.10	7.61	2.78	4.33	5.62	0.26	0.41
0.	6.98	5.96	3.15	3.54	6.13	0.32	0.48
0.10	9.09	3.53	4.01	2.50	7.39	0.45	0.70
0.20	11.62	1.76	5.03	1.88	8.94	0.60	1.03
0.30	14.48	0.44	6.15	1.48	10.68	0.76	1.48
0.40	17.76	-0.65	7.40	1.20	12.66	0.93	2.09
0.50	21.16	-1.52	8.68	1.01	14.71	1.11	2.83
0.60	24.82	-2.29	10.03	0.87	16.89	1.30	3.75
0.69	28.41	-2.90	11.34	0.76	19.01	1.48	4.76
0.80	32.44	-3.49	12.79	0.67	21.37	1.67	6.02
0.90	36.44	-3.99	14.22	0.60	23.69	1.87	7.42
1.00	40.44	-4.43	15.63	0.55	26.01	2.06	8.95
1.50	61.22	-6.14	22.87	0.37	37.87	3.03	19.05
2.00	82.87	-7.31	30.28	0.28	50.05	4.03	33.33
2.42	101.52	-8.05	36.61	0.23	60.46	4.87	48.67
2.99	126.67	-8.80	45.09	0.19	74.42	6.01	73.78
4.00	171.28	-9.71	60.05	0.14	99.05	8.01	130.80
5.00	216.14	-10.31	75.03	0.11	123.73	10.01	204.16
6.00	261.04	-10.75	90.00	0.09	148.40	12.01	293.70
6.99	305.68	-11.07	104.85	0.08	172.88	14.00	398.64
7.99	350.51	-11.31	119.76	0.07	197.45	15.99	520.03
10.00	441.30	-11.67	149.93	0.06	247.18	20.02	815.00

Table II. Parameters and characteristic integrals of the equilibrium solution.

REFERENCES

1. Michel, R., C. Quémard and R. Durant. Hypothesis on the Mixing Length and Application to the Calculation of the Turbulent Boundary Layers. Conference on Turbulent Boundary Layer Prediction, AFOSR - IFP, Vol. 1, Stanford, 1968.

2. Coles, D. and C. Hirst. Conference on Turbulent Boundary Layer Prediction, Vol. 2 (Compiled Data). AFOSR - IFP, Stanford, 1968.

3. Van Driest, E.R. On Turbulent Flow Near a Wall. Journ. of the Aeron. Sc. Vol. 23, Nov., 1956.

4. Clauser, F. Turbulent Boundary Layers in Adverse Pressure Gradients. Journ. of the Aeron. Sc., Vol. 21, 1954.

5. Rotta, J. Über die theorie der turbulenten Grezschichten (Theory of Turbulent Boundary Layers). Mitteilungen aus dem M.P.I. für Stromungsforschung, No. 1, Göttingen, 1950.

6. Bradshaw, P. and D. Ferris. The Response of a Retarded Equilibrium Turbulent Boundary Layer to the Sudden Removal of Pressure Gradient. The Turbulence Structure of Equilibrium Boundary Layers. N.P.L. Aero. Rep. 1145 (1965) and 1184 (1966).

7. Herring, H. and J. Norbury. Some Experiments on Equilibrium Turbulent Boundary Layers in Favorable Pressure Gradients. Journ. of Fluid Mechanics, Vol. 27, 1967.

8. Stratford, B.S. An Experimental Flow With Zero Skin-Friction Throughout its Region of Pressure Rise. Journ. of Fluid Mechanics, Vol. 5, 1959.

9. Mellor, G.L. and D.M. Gibson. Equilibrium Turbulent Boundary Layers. F.L.D., No. 13, Princeton University, 1963.

10. Schubauer, G.S. and P. Klebanoff. Investigation of Separation of the Turbulent Boundary Layers. N.A.C.A. TN 2133, 1950.

11. Head, M.R. Entrainment in the Turbulent Boundary Layer. Aeronautical Research Council, R.M. 31-52, 1958.

12. Stevenson, T.N. Experiments on Injection Into an Incompressible Turbulent Boundary Layer. College of Aeronautics, Cranfield, Rep. Aero, No. 177.

13. Mickley, H.S. and R.S. Davis. Momentum Transfer for Flow Over a Flat Plate With Blowing. N.A.C.A. TN 4017, 1957.

14. Favre, A., R. Dumas, E. Verollet and M. Coantic. Couche limite turbulente sur paroi poreuse avec aspiration (Turbulent Boundary Layer on a Porous Wall With Suction). A.G.A.R.D. Meeting: Recent Developments in Boundary Research, Naples, 1965.

15. Michel, R., C. Quémard and M. Elena. Distributions de vitesses des couches limites turbulentes en écoulement compressible uniforme ou accéléré. (Velocity Distributions in Turbulent Boundary Layers in Uniform or Accelerated Compressible Flow). Aeronautical Research, No. 128, Jan. - Feb., 1969.

16. Cohen, C.B. and E. Reshotko. Similar Solutions for the Compressible Laminar Boundary Layer With Heat Transfer and Pressure Gradient. N.A.C.A. TR 1293, 1956.

Translated for National Aeronautics and Space Administration under Contract No. NASw-2035, by SCITRAN, P. O. Box 5456, Santa Barbara, California, 93013.